Canadian Mineralogist
Vol. 26, pp. 355-376 (1988)

COEXISTING GALENA, PbS_{ss} AND SULFOSALTS: EVIDENCE FOR MULTIPLE EPISODES OF MINERALIZATION IN THE ROUND MOUNTAIN AND MANHATTAN GOLD DISTRICTS, NEVADA

EUGENE E. FOORD AND DANIEL R. SHAWE
M.S. 905, U.S. Geological Survey, Box 25046, Denver Federal Center, Lakewood, Colorado 80225, U.S.A.

NANCY M. CONKLIN
M.S. 928, U.S. Geological Survey, Box 25046, Denver Federal Center, Lakewood, Colorado 80225, U.S.A.

ABSTRACT

Studies of galena and Pb–Bi–Ag–Cu(Hg) sulfosalts of varied compositions in the Round Mountain and Manhattan gold districts of Nevada corroborate the occurrence of several distinct mineralized systems characterized by different mineral compositions and assemblages. The different episodes of mineralization are related to different Cretaceous and Tertiary magmatic–hydrothermal events, although the assignment of specific mineral compositions and associations with dated mineralized systems is still incomplete. At the Fairview mine, galena associated with Pb–Bi–Ag sulfosalts and simple sulfides occurs as intergrowths of discretely different composition controlled by silver and bismuth content. A galena-type phase (PbS_{ss}) with solid solution toward matildite, $AgBiS_2$ (composition $Gal_{60}Mat_{40}$) was found. If silver and, to a lesser extent, bismuth are absent, the galena formed will be almost pure PbS. Some minor antimony may substitute for bismuth. This study confirms a linear relationship between *a* cell edge and Ag–Bi(Sb) content for galena containing less than about 15 wt. % Ag and Bi(Sb). Other Pb–Bi–Ag–Cu(Hg) sulfides and sulfosalts identified from the districts are bismuthinite, galenobismutite, lillianite–gustavite, aikinite, friedrichite(?), hammarite, ourayite, and berryite(?). Phases X and Y, mercury-bearing Pb–Bi–Ag–Cu sulfosalts (most likely new species), and coloradoite were recognized from the Outlaw prospect southeast of Round Montain. Multiple episodes of mineralization are supported by: (i) coexisting galena, PbS_{ss} and complex sulfosalts of widely varied compositions and with textures that indicate successive replacement; (ii) a characteristic but commonly incomplete paragenesis of mineral species (early hübnerite, molybdenite, galena, sphalerite, and chalcopyrite; intermediate galena and Pb–Bi–Ag sulfosalts; late tetrahedrite–tennantite, galena(?), chalcopyrite(?), covellite, and mercurian minerals), some of which can be geologically or geochemically correlated with dated deposits; and (iii) mineral compositions as indicators of temperature of deposition (Sb:Bi <0.06, *T* 200–300°C; Sb:Bi >6.0–13, *T* 100–160°C).

Keywords: galena, PbS_{ss}, Pb–Bi–Ag–Cu(Hg) sulfosalts, Round Mountain, Manhattan, Nevada.

SOMMAIRE

Nos études de galène et des sulfosels de Pb–Bi–Ag–Cu(Hg) à composition variable, provenant des districts aurifères de Round Mountain et de Manhattan, au Nevada, confirment la présence de plusieurs épisodes distincts de minéralisation, dont témoignent les différents champs de composition et assemblages de minéraux. Si les épisodes de minéralisation sont liés à divers événements magmatiques-hydrothermaux, d'âge crétacé à tertiaire, en revanche l'attribution de compositions et d'associations spécifiques à des événements de minéralisation d'âge connu demeure incomplète. À la mine Fairview, la galène associée aux sulfosels Pb–Bi–Ag et aux sulfures simples se trouve en intercroissances dont la composition globale définit des regroupements en termes de teneur en argent et en bismuth. Nous avons trouvé une composition intermédiaire de galène (PbS_{ss}, $Gal_{60}Mat_{40}$) enrichie dans le terme matildite $AgBiS_2$. Si l'argent et, à un degré moindre, le bismuth sont absents, la galène formée par exsolution est par contre presque stoechiométrique. L'antimoine, en faibles quantités, peut remplacer le bismuth. Ces résultats confirment la relation linéaire entre le paramètre réticulaire *a* et la proportion de Ag–Bi(Sb) dans la galène pour des teneurs (en poids) inférieures à 15% Ag + Bi(Sb) environ. On a pu identifier d'autres sulfures et sulfosels de Pb–Bi–Ag–Cu(Hg): bismuthinite, galenobismutite, lillianite–gustavite, aikinite, friedrichite(?), hammarite, ourayite, et berryite(?). On signale la présence des phases *X* et *Y*, sulfosels de Pb–Bi–Ag–Cu mercurifères, qui sont probablement de nouvelles espèces, ainsi que la coloradoïte, dans l'indice minéralisé de Outlaw, au sud-est de Round Mountain. Les facteurs suivants indiquent qu'il s'agit d'une multiplicité d'épisodes de minéralisation: (i) une coexistence de galène, de PbS_{ss}, et de sulfosels complexes à compositions très variables et à textures qui indiquent une succession d'épisodes de remplacement; (ii) une paragenèse caractéristique mais typiquement incomplète de minéraux: hubnerite, molybdénite, galène, sphalérite et chalcopyrite (précoces), galène et sulfosels Pb–Bi–Ag (intermédiaires), et tétraédrite-tennantite, galène(?), chalcopyrite(?), covelline et minéraux de mercure (tardifs); dans certains cas, des corrélations géologiques et géochimiques sont possibles avec des gîtes minéraux dont l'âge est connu; et (iii) les indicateurs de température de formation à partir des compositions minérales (Sb:Bi <0.06, T 200–300°C; Sb:Bi > 6.0–13, T 100–160°C).

(Traduit par la Rédaction)

Mots-clés: galène, PbS_{ss}, sulfosels Pb–Bi–Ag–Cu(Hg), Round Mountain, Manhattan, Nevada.

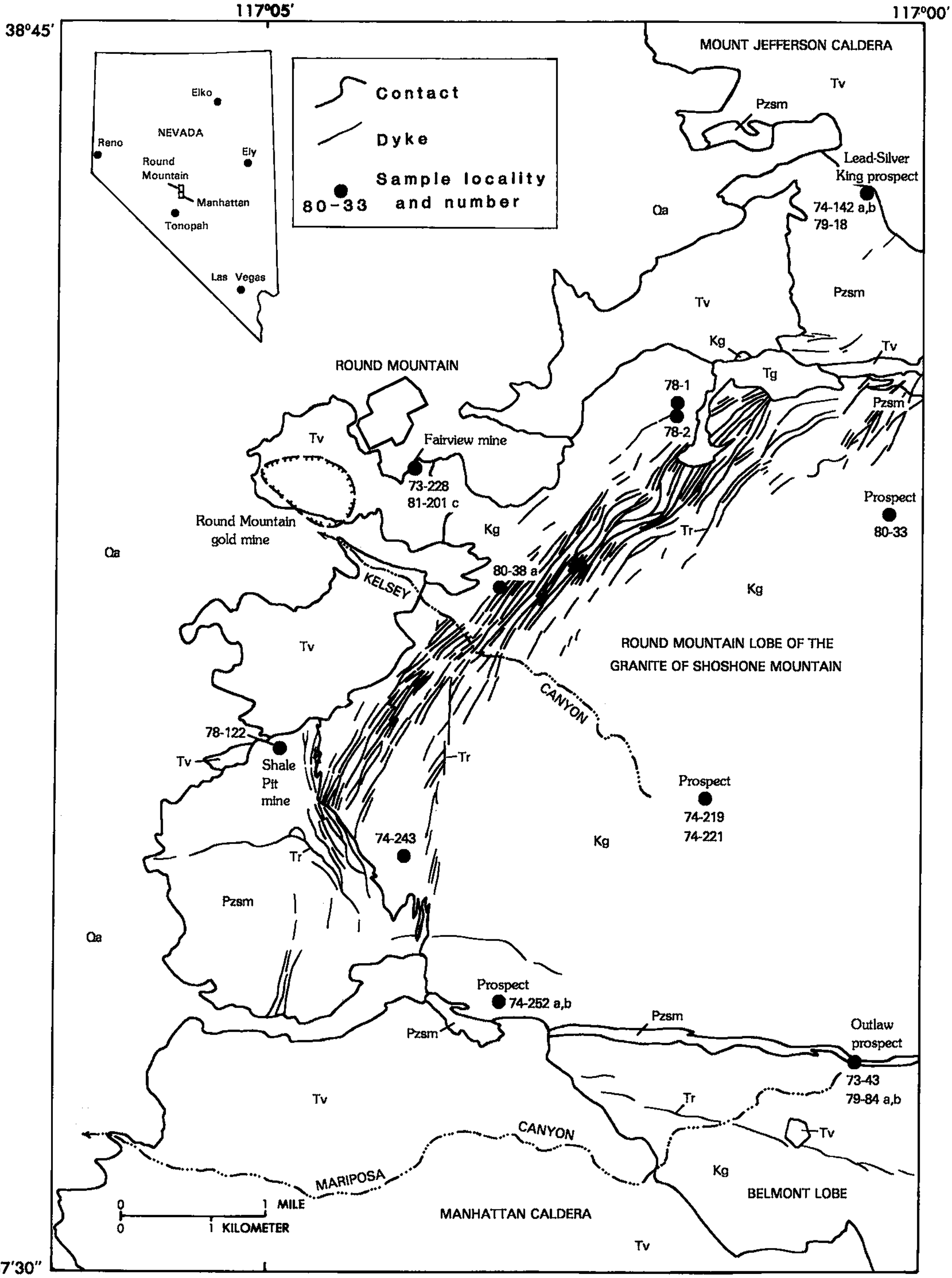

FIG. 1. Simplified geologic map of the Round Mountain quadrangle, showing locations of areas studied. Qa, Quaternary alluvium; Tv, Tertiary volcanic rocks (~24–27 Ma); Tg, Tertiary granodiorite stock (35 Ma); Tr, Tertiary rhyolite dykes (35 Ma); Kg, Cretaceous granite (~80–95 Ma); Pzsm, Paleozoic sedimentary and metamorphic rocks.

INTRODUCTION

As a part of the detailed geological mapping and mineral resource appraisal of the southern Toquima Range, Nye County, Nevada, the mineralogy and parageneses of the sulfides and coexisting Pb–Bi–Ag–Cu sulfosalts from many of the mines and prospects in the area were investigated (Figs. 1, 2). Physically and chemically different generations of galena and sulfosalts have been recognized. In addition, field mapping, radiometric dating, and petrographic and geochemical studies indicate a complex sequence of igneous activity and multiple episodes of mineralization (Shawe 1985, 1986, Shawe *et al.* 1986). These studies collectively have clarified the geological history of several mineral deposits in the area, in particular the large gold-silver deposit at Round Mountain.

GEOLOGY OF THE LOCALITIES STUDIED

The southern Toquima Range, in which the Round Mountain and Manhattan gold districts occur, is an area of complex geology that evolved over a long period of time. Paleozoic marine sedimentary rocks consist of Cambrian and Ordovician mostly transitional facies argillite, quartzite, and carbonate that were fault-thrust eastward as the Roberts Mountains allochthon during the late Devonian to Mississippian Antler orogeny. Other thrust-fault events followed in later Paleozoic and Mesozoic times, and they terminated when granitic plutons were emplaced into the sedimentary rocks in the Cretaceous. Tertiary igneous activity involved emplacement of stocks and dykes, and formation of several calderas accompanied by eruption of voluminous silicic ash-flow tuffs. Hydrothermal mineral deposits were formed or

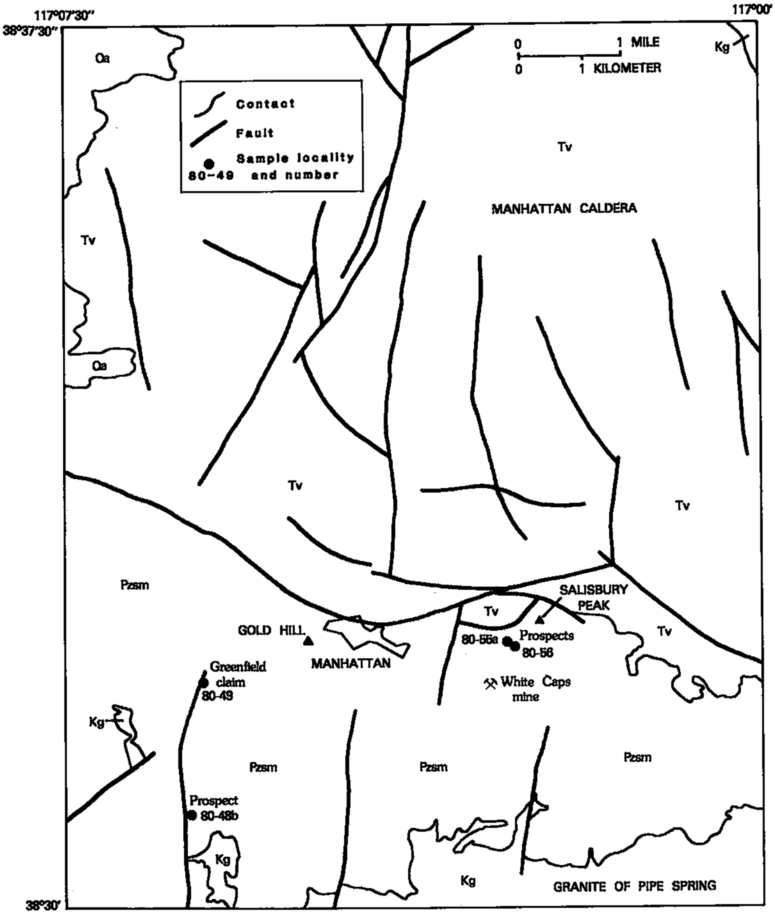

FIG. 2. Simplified map of the Manhattan quadrangle, showing locations of areas studied. Legend as on Figure 1.

remineralized in association with emplacement of the various igneous bodies. Locations of each of the mines and prospects examined are shown on Figures 1 and 2.

Following emplacement of granite plutons, a variety of small, mostly uneconomic base- and precious-metal veins and tungsten-bearing tactite and vein deposits formed at 75–80 Ma in the granite and in nearby Paleozoic carbonate and clastic rocks. The tactite and vein deposits characteristically contain pyrite, sphalerite, galena, and chalcopyrite as initial components. Other sulfide and sulfosalt minerals in the deposits appear to be the products of younger mineralizing events on the basis of textural critera. For example, tetrahedrite–tennantite typically fills vugs in quartz, is molded around early sulfide minerals, or fills fractures in broken sulfide mineral grains in some of the quartz veins. Tungsten-bearing veins in granite were remineralized with copper, lead, zinc, arsenic, and antimony in the vicinity of a 35 Ma granodiorite stock and associated rhyolite dyke-swarm. Tourmaline mineralization of granite and rhyolite dykes accompanied emplacement of the stock. The main gold–silver mineralization at Round Mountain occurred at 25 Ma within a rhyolitic ash-flow tuff. An economically significant gold–silver mineralizing event at Manhattan took place at 16 Ma within Paleozoic phyllitic argillite, quartzite, and carbonate along the south margin of the Manhattan caldera. A separate but undated Tertiary mineralizing event introduced mercury, antimony, and arsenic minerals into the eastern part of the Manhattan belt. The mercury mineralization produced a few small mineable deposits; it was widespread, and overlapped older zones of base- and precious-metal veins.

Fairview mine

The Fairview mine lies at the eastern edge of a mineralized zone in rhyolitic tuff that contains the large 25 Ma gold–silver deposit at Round Mountain. The Fairview mine produced gold mostly from thin stringers in sheared rock parallel to a west-northwest-striking fault, not far above a depositional contact of tuff on granite and Paleozoic rocks. These oxidized bodies contained gold associated with iron oxides (from pyrite) in drusy quartz, as well as gold plates interspersed in mosaic-textured vein quartz (Ferguson 1921). Judged from materials on the waste dumps at the Fairview mine, mining extended downward from veins and stringers in rhyolitic tuff into the underlying granite, where thin quartz veins were encountered. The vein material, texturally like nearby 80 Ma base- and precious-metal and tungsten-bearing veins in granite (Shawe *et al.* 1984), contains hübnerite, molybdenite, pyrite, multiple generations of covellite, bismuthinite, and ourayite, all as fillings of vugs and fractures in mosaic-textured to drusy quartz. Pyrite contains sparse tiny cubes of galena, and galena likewise contains rare tiny cubes of pyrite, suggesting possible contemporaneous formation of the minerals. Sulfosalt minerals are molded around broken grains of pyrite and molybdenite flakes. Covellite occurs as a replacement of and a fracture filling in galena. Muscovite fills shears in quartz and lines vein margins, and sparse hübnerite occurs as tiny, 1- to 2-mm-long crystals embedded in massive white vein quartz. Limonite is a common alteration mineral at the Fairview mine. Anglesite and cerussite are weathering products of galena.

Lead–Silver King prospect

The Lead–Silver King prospect lies in a zone of base- and precious-metal mineral deposits along the southwestern margin of the Mount Jefferson caldera. An intensely sheared, mineralized zone a few meters wide, along a northwest-trending fault that separates Ordovician carbonate rocks from a large horse of Tertiary rhyolite tuff, is about 100 m outside the caldera. Irregular, thin quartz veins in the sheared zone contain galena as irregular masses as much as several cm long, either as fillings of sheared milky quartz, or as crudely tabular masses in quartz-lined vugs. The quartz in vugs commonly is broken and healed. Cleavage surfaces of some galena masses are notably curved. As seen in polished section, some galena displays minute veinlets of marcasite, most commonly oriented along the cleavage planes. Oxidation products in the galena-bearing quartz veins include limonite, beudantite, and cerussite.

Prospect southeast of Round Mountain

An unnamed prospect shaft in granite of the Round Mountain lobe of the granite of Shoshone Mountain (Shawe 1981a) about 2 km southeast of Round Mountain exposes 3 or 4 closely spaced northeast-trending nearly vertical quartz veins 1–20 cm wide. The quartz-vein material, in appearance typical of the 80 Ma veins, contains pyrite, sphalerite, stibnite, and aikinite. Veinlets of covellite occur in the sulfides and sulfosalts. Alteration products of aikinite are abundant medium-yellow ocherous bismutite and minor anglesite. Locally, tabular masses of limonite derived from pyrite are as much as 3 cm thick and line vein margins. Sericitized granite wallrock contains small disseminated grains of pyrite and molybdenite, and sparse thin veinlets of pyrite. The prospect lies within 80 m of a northeast-trending rhyolite dyke of the 35 Ma swarm.

Fission-track ages determined on accessory zircon and apatite from pyrite-bearing granite collected near the quartz veins are about 43–44 Ma and 20 Ma, respectively (Shawe *et al.* 1986). The ages are interpreted to reflect partial annealing of zircon during emplacement of the 35 Ma dykes, and annealing of apatite probably during both the 35 Ma event and during the 25 Ma mineralization at nearby Round Mountain, followed by slow cooling to about 20 Ma at which time apatite had passed through the annealing threshold. Remineralization of the quartz veins may have occurred during either or both of these events.

The Shale Pit

The Shale Pit is a small gold mine in Ordovician carbonaceous argillite and limestone about 3 km south of the Round Mountain gold–silver mine. Gold mineralization occurred mostly in argillite just below a thrust fault that places limestone above the argillite. Very fine-grained gold is disseminated in silicified argillite where iron oxides (altered from pyrite) are abundant. Anomalous amounts of arsenic, antimony, mercury, and silver, along with other metals, suggest a kinship with Carlin-type gold deposits.

At the Shale Pit a pod of milky-white quartz about 2 m long occurs in strongly deformed silicified and iron-mineralized argillite about 3–5 m below the thrust fault that forms the sole of overlying limestone. The pod contains abundant masses of galena several cm long, interconnected by numerous thin anastomosing veinlets of galena. The galena displays somewhat curved cleavage surfaces. Thin veinlets in galena that are filled with cerussite contain sparse tiny grains of arsenopyrite. The quartz mass is strongly sheared and fractured, and locally it contains vugs lined with drusy quartz. The milky-white quartz of the pod appears typical of that in the 80 Ma veins; the drusy quartz is typical of the Tertiary gold-bearing deposits in the southern Toquima Range.

Prospect near the head of Kelsey Canyon

A prospect shaft 5 km southeast of Round Mountain near the head of Kelsey Canyon exposes a quartz vein, in granite, typical of the 80 Ma group of veins. The vein, of undetermined thickness, strikes northeast and dips steeply southeast. Vein material consists of massive milky-white quartz, but with locally abundant vugs into which less-milky quartz crystals extend.

Hübnerite occurs as isolated crystals in quartz and is partly altered to scheelite. Pyrite, galena, covellite, and tetrahedrite are seen mainly as vug fillings in quartz, and in irregular pockets formed in sheared quartz. Covellite forms irregular replacement patches and fills cleavages along crystallographic planes in galena (Shawe *et al.* 1984, Fig. 26), and tetrahedrite is molded around pyrite and galena crystals. Muscovite, barite, and fluorite occur as additional gangue minerals along with quartz. Anglesite is a weathering product of galena. Addition of sulfides to the vein, and alteration of hübnerite to scheelite, are thought to have occurred during a younger (35 Ma?) event following the initial (80 Ma) episode of hübnerite-bearing quartz vein mineralization (Shawe *et al.* 1984).

Prospect north of Mariposa Canyon

A prospect pit about 1.5 km north of Mariposa Canyon and 6.5 km south of Round Mountain exposes a quartz vein, in granite, that strikes N15°E and dips steeply west. A similar parallel vein lies 10 m west of the pit. The veins pinch and swell to a maximum thickness of about 0.5 m. They consist of mostly massive white quartz, but in places much vuggy quartz is evident. In one place a central fracture in the white massive quartz vein is lined with late vuggy quartz. Some vugs are lined or filled with chalcedony (Shawe *et al.* 1984, Fig. 25).

The veins contains sparse hübnerite embedded in massive quartz. Abundant sphalerite and lesser amounts of pyrite, galena, tetrahedrite–tennantite, and pyrrhotite(?) are concentrated in vugs in quartz, or are strung out in quartz close to or in prominent shears in the veins. The sphalerite contains tiny exsolved blebs of chalcopyrite (Shawe *et al.* 1984, Fig. 27). Chalcedony locally veins broken sphalerite crystals, and a late stage of quartz–chalcedony filled some vugs lined with quartz and pyrite crystals (Shawe *et al.* 1984, Figs. 24, 25). Tetrahedrite–tennantite, paragenetically younger than the early sulfides, shows late-stage alteration to chalcocite, acanthite, stromeyerite, covellite, and stibiconite(?) (Shawe *et al.* 1984, Fig. 28).

A quartz vein, which is in granite and is similar to the two veins at the prospect north of Mariposa Canyon and about 2.2 km to the northwest, and another one about 0.9 km to the north, have been dated as 78 and 79 Ma, respectively. Another quartz vein 0.5 km to the northwest, dated as 83 Ma, was sheared, brecciated, and remineralized in Tertiary time with chalcedony, barite, and cinnabar (data from Shawe *et al.* 1986).

Prospects north of White Caps mine

Prospects 0.7 km north-northeast of the White Caps mine east of Manhattan expose a set of quartz veins in Ordovician limestone on the south flank of Salisbury Peak. The veins are within about 300 m of the south margin of the Manhattan caldera, and they lie about 3 km north of a Cretaceous granite pluton, referred to as the granite of Pipe Spring (Shawe 1981b). Thin veins of white bull quartz a few cm to perhaps 1 m wide, generally northeast-trending and steeply dipping, occur where limestone is jasperized, calcsilicated, and iron-mineralized. Quartz is mostly massive and mosaic-textured, though locally it is vuggy. The quartz veins commonly exhibit thin selvages of muscovite, and in places potassium feldspar occurs with muscovite in vein selvages and extends into the cores of veins, forming a rock similar to pegmatite. Locally a few light-brown-weathering clots of calcite, no more than 1 cm across, and thin fracture fillings of calcite can be seen in white quartz. Sparse, small tabular masses of Pb–Bi–Ag sulfosalts along with minor chalcopyrite and galenobismutite occur in sheared quartz. Bismite(?), bismutite(?), or daubreeite–bismoclite(?) are alteration products of the sulfosalts.

The quartz veins at the prospects north of the White Caps mine are typical of veins associated with the granite plutons, though they show evidence of remineralization with complex sulfosalts. Similar quartz veins nearby have been dated at about 75 Ma. Also, the quartz veins at the prospects lie within a northeast-trending zone of Tertiary mercury mineralization centered on the White Caps mine.

Greenfield claim

Shallow prospect pits at the Greenfield claim about 2 km west-southwest of Manhattan expose thin irregular quartz veins in quartzite of the Ordovician Toquima Formation. The veins are about 2 km southwest of the margin of the Manhattan caldera and about 4 km northwest of the main mass of the granite of Pipe Spring (Shawe 1981b) south of Manhattan.

Silver- and bismuth-bearing galena occurs in quartz as well as in small (1 cm) masses along poorly defined irregular fractures in quartzite. Galena is the only sulfide mineral identified at this occurrence, although limonite in some of the vein material suggests the presence of pyrite at deeper levels where the rock has not been weathered. Cerussite is an alteration product of galena.

The Greenfield claim lies about 1 km south of the east-trending Manhattan belt of gold mineralization, and about 2 km west of the principal gold-producing zone on Gold Hill. Muscovite in quartz-mineralized rock at Gold Hill has been dated as 75 Ma, whereas adularia associated with gold at the same locality has an age of 16 Ma (Shawe *et al.* 1986).

Outlaw prospect

The Outlaw prospect, long known (Shannon 1924, Nuffield 1953, 1954, 1975, Karup-Møller 1972, 1977,

TABLE 1. SEMIQUANTITATIVE EMISSION-SPECTROGRAPHIC DATA FOR GALENA AND PbS_{ss} SAMPLES FROM THE ROUND MOUNTAIN AND MANHATTAN GOLD DISTRICTS, NYE COUNTY, NEVADA.

Locality	Fair-view mine	Lead-Silver King Prosp.		Shale Pit	Prospect, head of Kelsey Canyon		Prospect north of Mariposa Canyon		Green-field claim
Sample number	DRS 73-228	DRS-74-42a	DRS-79-18	DRS-78-122	DRS-74-221	DRS-74-219	DRS-74-252a	DRS-74-252b	DRS-80-49
	PbS_{ss}	PbS_{ss}	PbS	PbS_{ss}	PbS	PbS	PbS_{ss}	PbS_{ss}	PbS_{ss}
Fe	2000	1500	3000	150	30	50	<10	150	70
Mg	<50	<10	<10	<10	<10	100	<10	<10	10
Ca	100	30	<20	<20	30	<20	30	70	20
Ti	N1	N1	N1	N1	N1	20	N1	N1	N1
Mn	150	5	30	15	7	70	2	5	5
Ag	7%	0.7%	0.2%	1%	0.3%	0.3%	1.5%	2%	2%
Ba	70	7	30	70	70	15	30	30	300
Bi	>5%	>2%	.03%	1.5%	0.3%	0.3%	1.5%	2%	>2%
Cd	N10	150	150	150	N10	N10	300	70	150
Co	N10	N10	N10	N10	N10	N10	N10	N10	150
Cr	7	N10	L10	N10	N10	N10	N10	N10	N10
Cu	3000	10	20	50	1%	1.5%	1.5%	1.5%	700
Ni	N10	N10	N10	N10	N10	N10	N10	N10	15
Mo	3000	N5	N5	N5	N5	N5	7	7	N5
Pb	M	M	M	M	M	M	M	M	M
Sb	7000	N100	1500	3000	700	200	7000	N100	N100
Sn	70	N10	20	150	N10	N10	N10	N10	50
Sr	N5	30	15	150	15	10	5	N5	50
V	N	N	N		N	N	30	N	30
Si	3%	<10	<10	150	3000	5000	1.5%	3000	1500
Al	70	<10	<10	<20	150	3000	10	<10	<10
Na	N500	N500	N500	N500	N500	N500	N500	200	N500

Notes: N not detected at limit of determination. M Major. High Cu values in samples DRS-74-221, DRS-74-219, 74-252a and DRS-74-252b are due to admixed covellite. High Si values in these same four samples plus DRS-80-49 and DRS-73-228 are due to admixed quartz. N. M. Conklin, analyst. High values of Fe in samples DRS-73-228, DRS-74-142a, and DRS-79-18 are due to pyrite (or marcasite, or both) contamination; high value of Mo in sample DRS-73-228 is due to molybdenite contamination, and high Al in sample DRS-74-219 is due to contamination by minor feldspar. Values are in parts per million except for those indicated in %.

Harris & Chen 1975, 1976, Karup-Møller & Makovicky 1979, Makovicky & Mumme 1979, Dunning *et al.* 1988) as a locality for rare and complex Pb–Bi–Ag–Cu sulfosalts, is in a quartz vein at a contact between granite and schist about 8.5 km southeast of Round Mountain. The schist, representing metamorphosed sedimentary rocks of Ordovician(?) age, forms a narrow east-trending screen between two granite plutons (Shawe 1981a). The principal(?) vein is 1-2 m wide, strikes northeast, and dips steeply northwest, following an irregular contact between granite and schist. Vein quartz is milky white, generally mosaic-textured, and locally vuggy. The vein has been much sheared, and commonly shows thin lenses of granite or schist sheared into the vein margins. Muscovite forms thin selvages on the vein walls, as well as irregular lenses and blebs within quartz. Small tourmaline crystals line shears in quartz locally near tourmaline schist wallrock. Fluorite, pyrite, and rare rutile are intergrown with irregular masses of muscovite within quartz, or they occur as isolated crystals in quartz. The pyrite locally is granular to porous (or spongy), giving the appearance of having been corroded and leached. Sphalerite, galena, molybdenite, and several Pb–Bi–Ag–Cu sulfosalts occur as euhedral crystals and irregular masses in sheared vein quartz, and as fillings in vugs in quartz. The pyrite, sphalerite, galena, and molybdenite commonly are fractured, and the fractures filled with sulfosalts. According to Shannon (1924) chalcopyrite fills thin veinlets in benjaminite. A late generation of Hg-bearing Pb–Bi–Ag–Cu sulfosalts and coloradoite is also present. Limonite is a common alteration product, and anglesite and bismoclite–daubreeite(?) are present as alteration products of aikinite. Minor amounts of bismutite, sulfur, and cerussite also were identified as alteration products of aikinite (Dunning *et al.* 1988).

Muscovite from the quartz vein at the Outlaw prospect has an age of 81 Ma (Shawe *et al.* 1986), indicating that it was formed as part of the mineralization related to the Late Cretaceous granite plutons. However, the prospect lies in an east-trending belt of Tertiary mercury deposits that extends from south of Round Mountain for more than 10 km eastward (Shawe 1986). The leached pyrite in the deposit and veining of sulfides by sulfosalts suggest that at some time following formation of the base-metal deposit, additional hydrothermal activity occured. The presence of tourmaline suggests that the mineralization is related to the 35 Ma igneous episode.

MINERALOGICAL DATA

Results of our studies are organized in the following pages on the basis of mineral species and groups. Material from several localities in the Round Mountain and Manhattan gold districts provided data on galena, galena solid-solution (PbS_{ss}), and other sulfides specifically associated with the galena, on bismuthinite, galenobismutite, and berryite(?), on lillianite–gustavite and on tetrahedrite–tennantite. The Outlaw prospect near Round Mountain is discussed separately in considerable detail because of

TABLE 2. ELECTRON MICROPROBE DATA FOR COEXISTING GALENAS, PbS_{ss}, AND OURAYITE FROM THE ROUND MOUNTAIN - MANHATTAN AREA, NYE CO., NEVADA.

Locality	Fairview mine			Lead Silver King prospect		Shale Pit	Prospect head of Kelsey Canyon		Prospect north of Mariposa Canyon	Greenfield claim
Sample number	DRS-73-228 phase 1	phase 2	phase 3	DRS-74-142b	DRS-79-18	DRS-78-122	DRS-74-219	DRS-74-221	DRS-74-252b	DRS 80-49
No. of anal. points	6	2	2	5	4	5	4	3	3	2
min. name	ourayite	PbS_{ss}	PbS_{ss}	PbS	PbS	PbS_{ss}	PbS	PbS	PbS_{ss}	PbS_{ss}
Cu	0.0	0.0	0.0	0.0	0.0	0.0	0.0	0.0	0.0	0.0
Sb	0.9	0.1	0.2	0.1	0.3	0.3	0.0	0.1	0.0	0.1
Zn	0.0	0.0	0.0	0.0	0.0	0.0	0.0	0.0	0.0	0.1
S	16.0	14.3	14.9	13.4	13.4	13.4	13.5	13.3	13.5	13.8
Pb	39.5	70.8	56.7	86.9	86.2	87.0	87.5	85.5	83.3	81.2
Bi	33.3	9.1	18.5	0.0	0.0	0.2	0.0	0.0	1.6	3.1
Ag	9.6	4.8	9.4	0.0	0.1	0.5	0.1	0.2	0.9	1.7
Fe	0.0	0.0	0.2	0.0	0.0	0.0	0.0	0.0	0.0	0.0
As	0.2	0.0	0.0	0.0	0.0	0.0	0.0	0.0	0.0	0.0
Te	--	--	--	0.0	--	0.0	--	--	--	--
Total	99.5	99.1	99.9	100.4	100.0	101.4	101.1	99.1	99.3	100.0

Note: Mo and Hg sought in sample DRS-80-49 and found to be below the detection limit. Sample DRS-78-122 also contains 0.1% Se and 0.03% Te based on emission spectrographic analysis. -- Not determined.

TABLE 3. CONTENTS OF CHALCOPHILE ELEMENTS FOR SELECTED SAMPLES OF GALENA.

Locality	Lead-Silver King prospect		Shale Pit prospect	Prospect head of Kelsey Canyon
Sample number	DRS-74 -142a	DRS-79 -18	DRS-78 -122	DRS-74 -221
As	20	10	20	20
Au	<10	<0.2	<0.2	<0.4
Bi	1%(1.2)$^{+}$	200(170)$^{+}$	>0.2%(0.56)$^{+}$	1500(2300)$^{+}$
Cd	100(150)*	100(150)$^{+}$	150(150)$^{+}$	4(N)*
Sb	300 (N)*	1400(1500)*	>0.2%(0.3)*	400(700)*
Te	20	15	300	100
Zn	<20(N)*	6(N)*	100(N)*	40(N)*
P	<100	7	7	<2
Tl	<100	<1	10	2
Hg	500	H	H	H
Se	<500	200	1000	100

Notes: Values are given in ppm, and where stated, in wt. %. H = interference. For samples DRS-74-142a and DRS-78-122 the usual limits of detection do not apply because of the dilution factor. Chalcophile element spectrographic analyses by C. Heropoulos (USGS). * - values determined by regular six-step spectrographic analysis (N. M. Conklin, analyst). + - values determined by quantitative emission-spectrographic analysis (N. M. Conklin, analyst).

its historical importance and the wealth of mineralogical data that has been acquired for that locality. A brief section deals with alteration products of some sulfides and sulfosalts in the Round Mountain - Manhattan area.

Galena and galena solid-solution

Galena and PbS_{ss} from the Round Mountain - Manhattan area show a large variation in trace- and

TABLE 4. CONTENTS FOR SILVER, BISMUTH, AND ANTIMONY IN GALENAS.

Sample no. and locality	Element content Ag	Bi	Sb	Bi/Ag ratio (wt.) (from quant. spec. data)
DRS-79-18 Lead-Silver King Prosp.	1400 (1300)	170 (none)	1500^{+} (1400)* (2600)	0.05
DRS-74-142a Lead-Silver King Prosp.	6100 (---)	12000 (---)	N100^{+} (300)* (---)	2.0
DRS-74-142b Lead-Silver King Prosp.	(200) 1500	(<200) 700	(800)	
DRS-78-122 Shale Pit	5200 (5100)	5600 (3300)	3000^{+} (>2000)* (2600)	1.1
DRS-74-219 Prospect, head of Kelsey Canyon	(1200)	(200)	(400)	
DRS-74-221 Prospect, head of Kelsey Canyon	2200 (1800)	2300 (200)	700^{+} (400)* (600)	1.0
DRS-74-252a Prospect north of Mariposa Canyon	7500 (9000)	14000 (15700)	7000^{+} (400)	1.9
DRS-80-49 Greenfield claim	21000 (17100)	45000 (31300)	N100^{+} (600)	2.1

Notes- values for Ag and Bi not in parentheses are those determined by quantitative six-step emission spectrography (N. M. Conklin, analyst). * - values in parentheses for Sb are those determined by quantitative chalcophile element spectrography (C. Heropoulos, analyst). Microprobe values given in parentheses (E. E. Foord, analyst). + - values determined by regular six-step semiquantitative emission spectrography (N. M. Conklin, analyst). Discrepancy in microprobe and spectrographic values of Sb in sample DRS-74-252a unaccounted for. (---) - sample not examined by microprobe.

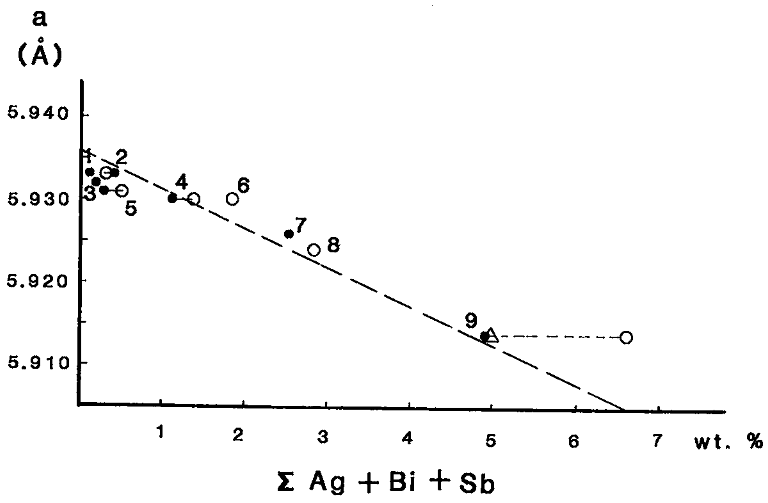

FIG. 3. Relation of *a versus* summation of Sb+Ag+Bi for galena from the Round Mountain - Manhattan area (1, DRS-74-142b; 2, 79-18; 3, 74-219; 4, 78-122; 5, 74-221; 6, 74-142a; 7, 74-252b; 8, 74-252a; 9, 80-49). Solid circle, by electron-microprobe; open circle, by quantitative emission spectrography. An additional data point (from Karup Møller & Makovicky 1981), is shown as an open triangle. All cell dimensions ±0.002 Å. Microprobe data are ±0.4 wt.%.

minor-element contents. Discrete coexisting galena and PbS_{ss} with different compositions have been identified from two localities (Lead–Silver King prospect and Fairview mine dump) and probably exist elsewhere as well (Foord *et al.* 1985). Tellurium and selenium substitution for sulfur in galena (altaite and clausthalite components, respectively) was determined to be nearly nil. Results of spectrographic and electron-microprobe analyses are given in Tables 1 and 2, respectively. Concentrations of chalcophile elements are shown in Table 3; those of silver, bismuth, and antimony in selected galena samples are given in Table 4.

Back-scattered electron (BSE) imaging of the galena from the Greenfield Claim (DRS-80-49) showed homogeneous-appearing galena, an unusual property for galena with such high content of bismuth and silver.

An almost linear correlation may be seen between the *a* cell edge and the sum of silver, bismuth, and antimony contents in galena samples (Fig. 3). Data from the literature are included for comparison. Figure 4 showns the compositions determined by electron microprobe and plotted along the galena–matildite join. It can been seen on this figure that some of the points show a slight excess in bismuth. This phenomenon suggested to Karup-Møller (1977) that the Bi-excess in galena may be due to domain-type structures similar to those in the lillianite homologues.

Because of the extremely small amount of PbS_{ss} and associated sulfides and sulfosalts collected from the Fairview mine dump, all data (X-ray, emission spectrographic and microprobe) could not be obtained on exactly the same grain or grains of material. A 114-mm diameter Gandolfi X-ray pattern made from a somewhat brittle silvery-white sulfide or sulfosalt associated with visible molybdenite and quartz in veins within hydrothermally altered granite (sample DRS-73-228, Fairview mine) shows

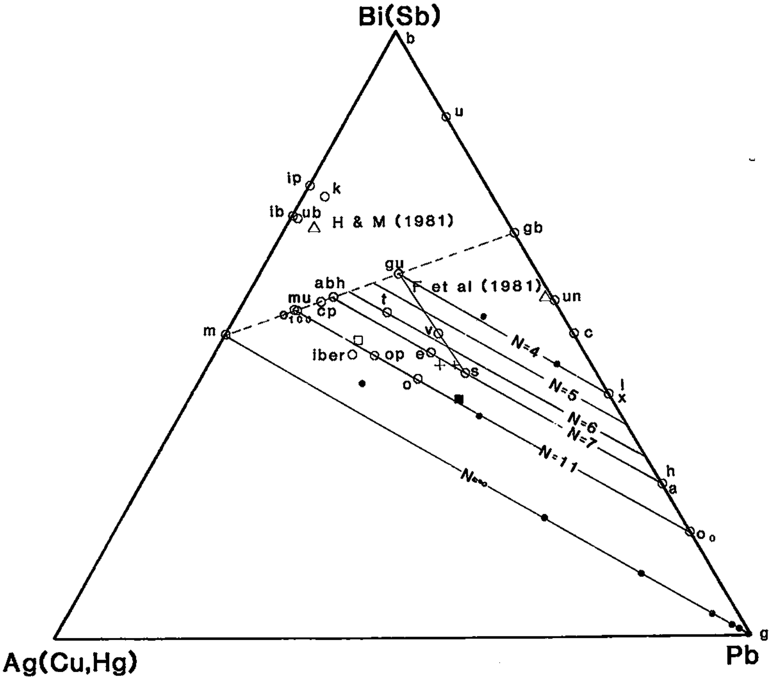

FIG. 4. Triangular plot in terms of *Pb, Bi(Sb),* and *Ag(Cu,Hg),* showing the compositions (atomic) of galena and associated sulfosalts from the Round Mountain – Manhattan area. Selected data from the literature are also shown. Symbols: open circle, known minerals and ideal compositions; solid circle, samples from Round Mountain and Manhattan; open square, Karup Møller (1977); open triangle, Finashin *et al.* (1981), Herbert & Mumme (1981); +, phase X; solid square, phase Y; b, bismuthinite; u, ustarasite; ip, ideal pavonite; ib, ideal benjaminite; ub, unsubstituted benjaminite; k, kitaibelite; gb, galenobismutite; gu, gustavite; abh, Ag-Bi heyrovskyite; mu, mummeite; cp, cupropavonite; o_{100}, ourayite$_{100}$; op, *P*-centered ourayite; t, treasurite; un, unnamed; c, cosalite; v, vikingite; iber, ideal berryite; m, matildite; e, eskimoite; o, ourayite (*B*-centered); s, schirmerite; l, lillianite; x, xilingoite; h, heyrovskyite; a, aschamalmite; g, galena.

lines that could be indexed on two discrete galena-type cells. However, after the discovery of an ourayite composition (Our_{53}) as well as that of PbS_{ss} by microprobe analysis of additional material, and BSE imaging indicated an intergrowth of two minerals, it was realized that one of the galenas was ourayite. Additional X-ray powder-diffraction studies of material from the prepared polished section also indicated the presence of ourayite. The X-ray-diffraction pattern of ourayite

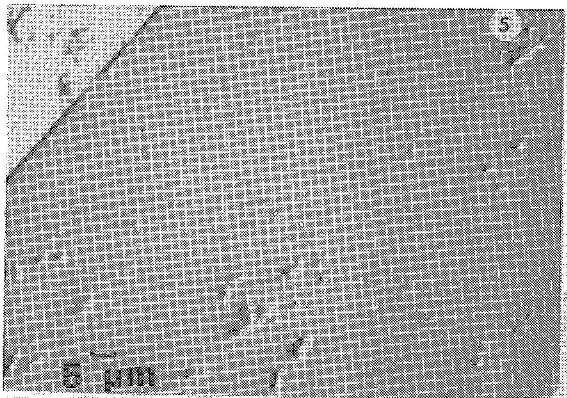

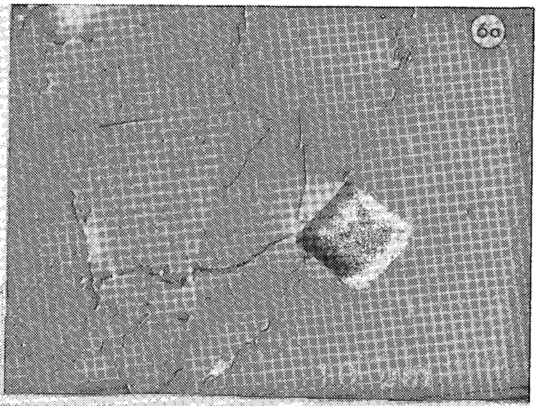

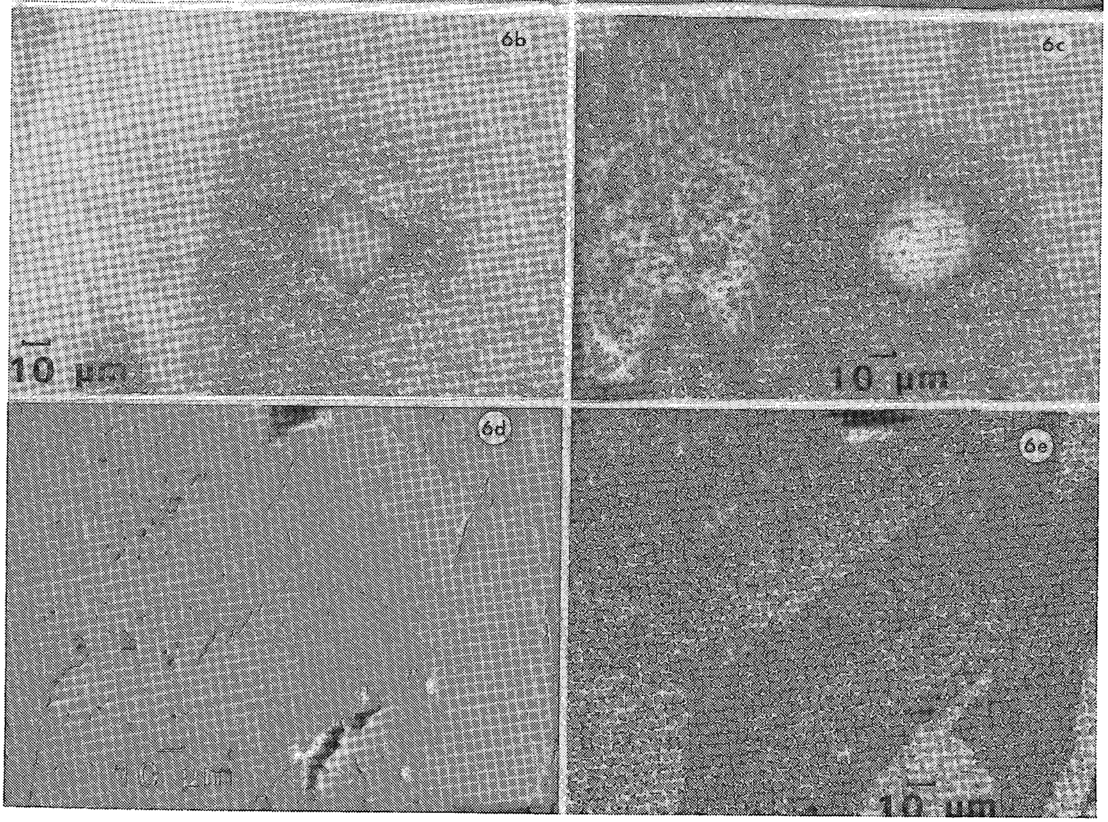

FIG. 5. Back-Scattered Electron (BSE) photograph of Gal_{60}-Mat_{40} (medium grey) and host pyrite (white) from the Fairview mine, Round Mountain, Nevada. Sample DRS-73-228.

FIG. 6. BSE, and element dot maps for an aggregate of minerals in sample DRS-73-228 (Fairview mine). (a) BSE image: pyrite, black cube; ourayite(?), dark grey; PbS_{ss}, light grey. (b) Pb*Mα* dot map, same area as on 6a. (c) Bi*Mα* dot map, same area as 6a and 6b. (d) BSE image: pyrite, black; ourayite(?), medium grey; PbS_{ss}, light grey. (e) Ag*Lα* dot map, same area as 6d.

(Karup-Møller 1977, Makovicky & Karup-Møller 1984) is similar to that of galena, owing to the presence of dominantly galena-type layers with relatively few bismuthinite-type layers. Single-crystal studies will be necessary to confirm whether the ourayite is *B*-centered or *P*-centered (Makovicky & Karup-Møller 1984) or if it is another mineral species having a value of N equal to 11. A lillianite homologue can be characterized by the number of octahedra (N) in the octahedral chains in each of two types of layers (Makovicky & Karup-Møller 1977a,b). On the basis of electron-microprobe analyses and SEM studies, two galena-type phases (phases 2 and 3) were found along with a dominant third phase (phase 1) compositionally most closely resembling ourayite. X-ray-diffraction studies of this material identified phases 1 and 2 as ourayite and galena, respectively. An insufficient amount of phase 3 (highest Ag- and Bi-containing galena) was present for detection by X-ray diffraction. However, careful examination of phase 3 ($\mathrm{Gal}_{60}\mathrm{Mat}_{40}$) at high magnification using SEM BSE imaging techniques showed no traces of any other intergrown or exsolved mineral phase (Fig. 5).

Annealing studies of two samples of the hand-picked fragments selected for spectrographic analysis, and which were initially determined to have two galena-type phases present (subsequently identified as an intergrowth of galena and ourayite), when heated at 500°C *in vacuo* for 1 week produced material that gave a sharper single galena-type pattern along with a faint pattern for ourayite. We conclude that the untreated sample contained, in addition to ourayite(?), two discrete compositions of galena, both of which contain abundant matildite in solid-solution (PbS_{ss}). Upon heating, the two different compositions of galena were homogenized, and the ourayite-like mineral was converted to the artificial equivalent of ourayite *sensu stricto*.

Figures 6a to 6e show BSE and selected-element dot maps for phases 1 (Our_{53}) and 2 ($\mathrm{Gal}_{80}\mathrm{Mat}_{20}$) in DRS-73-228 from the Fairview dump (Fig. 1). Simultaneous crystallization of ourayite, PbS_{ss}, and pyrite seems indicated; compositional boundaries between different minerals are sharp and no exsolution-type textures are visible. Phase 3 ($\mathrm{Gal}_{60}\mathrm{Mat}_{40}$) is totally enclosed within a grain of pyrite (Fig. 5).

An emission-spectrographic analysis of hand-picked fragments yielded the composition for DRS-73-228 given in Table 1. Three thousand ppm molybdenum are present, indicating somewhat less than 1% molybdenite contamination. X-ray-diffraction studies confirm the presence of minor amounts of 3*R* molybdenite and quartz. Three distinct sulfide and sulfosalt phases in addition to pyrite (Table 2, Fig. 4) were determined to be present based on optical and electron-microprobe studies.

Bismuthinite, galenobismutite, gustavite, and berryite(?)

A lead-bearing bismuthinite was identified in one sample (DRS-81-201c), collected from the Fairview mine dump south of Round Mountain (Fig. 1). The grey, metallic bismuthinite is associated with quartz and pyrite. A six-step semiquantitative emission-spectrographic analysis (by NMC) showed: Fe 0.15%, Mg <10 ppm, Ca <20 ppm, Ag 70 ppm, Bi major, Cu 0.7%, Nb 15 ppm, Pb 2%, Sb 0.3%, Zr 20 ppm, Si 0.3%, and Al <10 ppm. Other elements were not detected at their respective limits of determination. Chalcophile elements were also determined (by C. Heropoulos, USGS) for the sample with the following results (in ppm): As 100, Au <0.3, Bi >1000, Cd 4, Sb 200, Te 200, Zn 26, P <1, Tl <1, Hg <1, Se 1300.

An average of six electron-microprobe analyses gave: Bi 79.22 wt.%, Pb 2.23, S 18.47, total 99.92. A structural formula calculated on the basis of two cations is $(\mathrm{Bi}_{1.95}\mathrm{Pb}_{0.05})\mathrm{S}_{2.95}$, or if calculated on the basis of 3 sulfur atoms is $(\mathrm{Bi}_{1.97}\mathrm{Pb}_{0.06})\mathrm{S}_3$. This bis-

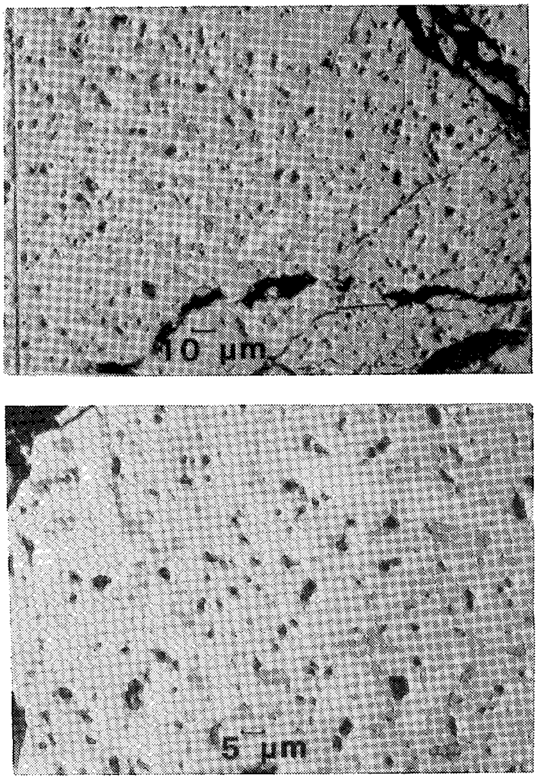

FIG. 7a. BSE photograph of intergrowth of gustavite, laths of bismuthinite and sparse patches of alteration products, prospect north of the White Caps mine (DRS-80-56). White, bismuthinite; light grey, gustavite; dark grey, galena. 7b. BSE closeup-photograph of 7a.

muthinite is similar in composition to others reported in the literature (Fig. 4). BSE photographs show the bismuthinite to be monomineralic.

One polished section (DRS-80-56) of vein quartz from one of the prospects north of the White Caps mine contains an intergrowth of Pb–Bi–Ag–Cu–Sb sulfosalts; X-ray, spectrographic, and electron-microprobe analyses show these to consist chiefly of bismuthinite, galenobismutite, and gustavite with lesser amounts of berryite(?). Cerussite, bismutite, bismite, and other alteration products are also present. BSE-imaging and EDS analysis of the finer grained part of the intergrowth show the presence of major gustavite enclosing randomly oriented laths of bismuthinite and scattered, extremely small anhedral blebs, patches and veinlets of alteration products within the gustavite (Fig. 7a). The bismuthinite laths are 5–10 μm long and 2–5 μ m wide. Alteration patches of cerussite and/or anglesite, and Bi-bearing minerals are typically 2 μm across (Figs. 7a,b). Another part of the same polished section contains a coarser grained (50–100 μm across) intergrowth of euhedral crystals of bismuthinite and galenobismutite without gustavite. A six-step emission-spectrographic analysis (NMC) of the mixture gave: Fe 700 ppm, Mg 10 ppm, Ca 200 ppm, Ag 2%, Ba 200 ppm, Be 2 ppm, Bi >10%, Cd 300 ppm, Co 7 ppm, Cu 1.5%, Ni 7 ppm, Pb >10%, Sb 5000 ppm, Si 1.5%, and Al <10 ppm. Other elements were not detected at their respective limits of determination (Table 5). The Si is from quartz contamination. Chalcophile elements determined spectrographically by C. Heropoulos, USGS, are: As 560 ppm, Au <1.6 ppm, Bi >1%, Cd 400 ppm, Sb 1600 ppm, Te 240 ppm, Zn 80 ppm, P <1 ppm, Tl 16 ppm, Hg 15 ppm, Se 2400 ppm.

TABLE 5. APPROXIMATE LOWER LIMITS OF DETERMINATION FOR ELEMENTS DETERMINED BY 6-STEP SPECTROGRAPHIC METHOD (IN PERCENT AND PPM)

Si	0.002%	Ga	5 ppm	Sr	5 ppm
Al	.001	Gd	50	Sm	100
Fe	.001	Ge	10	Ta	200
Mg	.002	Hf	100	Tb	200
Ca	.002	Ho	20	Te	2000
Na	.05%	In	10 ppm	Th	200 ppm
K	.7	Ir	50	Tl	50
Ti	.0002	La	30	Tm	20
P	.2	Li	50	U	500
Mn	.0001	Lu	30	V	7
Ag	0.5 ppm	Mo	3 ppm	W	100 ppm
As	1000	Nb	10	Y	10
Au	20	Nd	70	Yb	1
B	20	Ni	5	Zn	200
Ba	1.5	Os	50	Zr	100
Be	1 ppm	Pb	10 ppm		
Bi	10	Pd	10		
Cd	20	Pr	100		
Ce	150	Pt	30		
Co	3	Re	30		
Cr	1 ppm	Rh	2 ppm		
Cu	1	Ru	10		
Dy	50	Sb	150		
Er	50	Sc	5		
Eu	100	Sn	10		

An average of three microprobe analyses of the galenobismutite gave: Cu 0.2, Sb 0.1, S 17.1, Pb 27.5, Bi 56.2 , total 101.1 wt.%. Zinc, arsenic, iron, and silver were sought but were found to be below the limits of detection. This material is normal galenobismutite; its composition is plotted on Figure 4.

An average of six electron-microprobe analyses of the bismuthinite gave: Bi 80.63, Pb 1.45, S 18.42, total 100.50 wt.%. A calculated structural formula based on 3 S atoms is: $(Bi_{2.01}Pb_{0.04})S_3$.

The gustavite matrix enclosing laths of bismuthinite is uniform in appearance (BSE images) and is homogeneous in composition. An average of six microprobe analyses is given in Table 6.

A fourth mineral, which may be berryite, is associated with the gustavite, bismuthinite, and galenobismutite in DRS-80-56. The chemical formula of berryite still is uncertain, and the extent of solid-solution between copper and silver end-members is variable. An electron-microprobe analysis of one grain of the berryite(?) gave: Cu 5.11, Sb 0.86, S 16.55, Pb 24.61, Bi 42.32, Ag 10.09, total 99.54 wt.%. Zinc, arsenic, and iron were sought but not detected. If the data are recast on the basis of 16 S atoms, the formula is: $Pb_{3.8}(Ag_{3.0}Cu_{2.6})(Bi_{6.4}Sb_{0.3})S_{16}$; on the basis of 11 S atoms, the formula is: $Pb_{2.6}(Ag_{2.0}Cu_{1.8})(Bi_{4.4}Sb_{0.2})S_{11}$. If the mineral is berryite then some minor substitution of antimony for bismuth is likely. No X-ray-diffraction studies on pure material were done because of the small grain-size. A Gandolfi film for a sample of bulk material showed major bismuthinite, lesser galenobismutite and gustavite, plus additional faint lines that are close to those of berryite. The composition of the probe-analyzed berryite(?) material is shown on Figure 4. Ideal berryite is also plotted on the Figure. Other analyzed samples (Nuffield & Harris 1966, Karup-Møller 1966, 1977, Borodayev & Mozgova 1971, Harris & Owens 1973) are shown on Figure 8. Berryite is the only phase that is close in composition to our analyzed material.

TABLE 6. ELECTRON MICROPROBE DATA FOR LILLIANITE AND GUSTAVITE FROM MANHATTAN, NEVADA

	DRS-80-55A Lillianite	DRS-80-56 Gustavite
	Average of 7	Average of 6
Cu	0.0	0.1
Sb	0.2	.3
S	16.3	16.45
Pb	42.3	31.9
Bi	39.2	47.8
Ag	2.2	5.4
As	0.1	---
Te	0.2	.1
Total	100.4	102.05

Note: Zn and Fe sought but not detected. --- not determined.

Lillianite–gustavite series

Studies of members of the lillianite–gustavite ($Pb_3Bi_2S_6$ - $PbAgBi_3S_6$) series (*e.g.*, Nedachi *et al.* 1973, Makovicky & Karup-Møller 1977b, Finashin *et al.* 1981) have indicated a solid-solution series between the two minerals with a miscibility gap in the series between about Gus_{50} and Gus_{85}.

Blades of lillianite enclosed in quartz comprise sample DRS-80-55a from one of the prospects north of the White Caps mine. An average of seven microprobe analyses is shown in Table 6. Five 114 mm Gandolfi X-ray-diffraction films of the lillianite in DRS-80-55a showed the material to be mostly lillianite, with a trace of galena. The galena was not found during the microprobe analyses of the lillianite. The lillianite in DRS-80-55a ranges in composition from $L_{74}Gus_{26}$ to $L_{76}Gus_{24}$ (Fig. 4), following the nomenclature of Makovicky & Karup-Møller (1977a,b). The calculated N_{chem} is equal to 3.99. The gustavite from DRS-80-56 has an average composition of $L_{39}Gus_{61}$ and appears to be compositionally homogeneous (Table 6).

As stated by Makovicky & Karup-Møller (1977b), natural phases belonging to the lillianite–gustavite series, $Pb_3Bi_2S_6$ - $PbAgBi_3S_6$, are homogeneous between Gus_{100} and Gus_{85} (the 8-Å phases) and again between Gus_{50} and Gus_0 (the 4-Å phases; *e.g.*, Ontoyev *et al.* 1982). High-temperature phases with compositions situated in the compositional gap show exsolution phenomena. The lillianite in DRS-80-55a is homogeneous and represents lower temperatures of crystallization than the crest of the solvus. Because the gustavite in sample DRS-80-56 appears homogeneous (BSE imaging) even at high magnification (2000×), it may have cooled rapidly enough

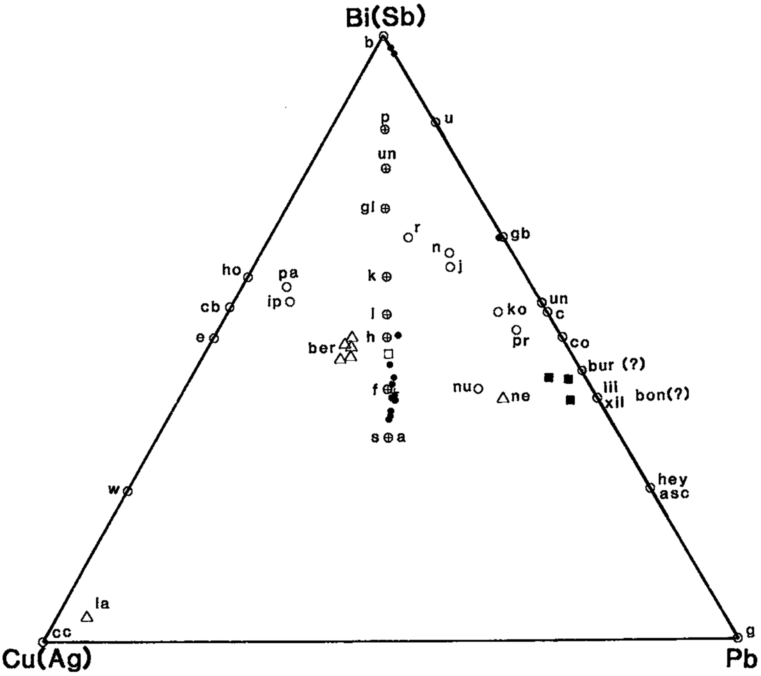

FIG. 8. Triangular plot in terms of *Cu(Ag)*, *Pb*, and *Bi(Sb)* showing the compositions (atomic) of aikinite–bismuthinite series minerals and others. Solid circle, compositions of minerals from Round Mountain – Manhattan; plus sign, average of compositions of seven samples from the Outlaw prospect; open circle with cross, aikinite–bismuthinite series; open circle, other natural minerals; open triangle, unknown structure; open square, Karup Møller (1977); b, bismuthinite; p, pekoite; u, ustarasite; un, unnamed; gl, gladite; r, rezbanyite; n, nordstromite; j, junoite; k, krupkaite; gb, galenobismutite; pa, paderaite; ho, hodrushite; cb, cuprobismutite; e, emplectite; l, lindströmite; ip, ideal paderaite; h, hammarite; ber, berryite; ko, kobellite; pr, proudite; c, cannizarite; co, cosalite; bur(?), bursaite; lil, lillianite; xil, xilingoite; bon(?), bonchevite; hey, heyrovskyite; asc, aschamalmite; g, galena; w, wittichenite; la, larosite; cc, chalcocite; f, friedrichite; s, soucekite; a, aikinite; nu, nuffieldite; ne, neyite; solid squares, giessenite. Bonchevite and bursaite are inadequately described minerals.

TABLE 7. CHALCOPHILE ELEMENT CONCENTRATIONS IN THREE SAMPLES OF TETRAHEDRITE FROM THE ROUND MOUNTAIN AREA

Sample nos.	DRS-78-1	DRS-78-2	DRS-74-243
	(For locations see Shawe et al. 1984)		
Element			
As	>2000	>2000	700
Au	0.5	<0.2	2
Bi	200	20	>1000
Cd	>1000	50	>1000
Sb	>2000	>2000	>2000
Te	100	100	100
Zn	>200	>200	>200
P	<1	<1	<1
Tl	<1	<1	<1
Hg	50	20	50
Se	20	<5	<5

Analyst C. Heropoulos (U.S. Geological Survey). Data obtained by emission spectrography.

to prevent exsolution at a scale large enough to be visible.

Tetrahedrite–tennantite

Arsenic-poor to moderately arsenic-bearing tetrahedrite, as determined by electron-microprobe analysis, is a minor but widespread constituent of many of the 80 Ma quartz–hübnerite–muscovite veins, which were remineralized by later hydrothermal events in the Round Mountain - Manhattan area (Shawe *et al.* 1984). Concentrations of chalcophile element for three tetrahedrite grains are given in Table 7. One sample of antimony-bearing tennantite (DRS-80-48b), which is from a mineralized thrust zone 2 km southwest of Manhattan associated with quartz, pyrite, galena, and secondary covellite and stibiconite(?) also was examined by electron microprobe. The maximum amount of silver determined by electron-microprobe analysis to be present in any of the six examined tetrahedrite-tennantite samples from the Round Mountain - Manhattan area is about 3%.

TABLE 8. MINERALOGY OF THE OUTLAW PROSPECT, MARIPOSA CANYON, TOQUIMA RANGE, NEVADA

Mineral	References
Quartz	1, 2, 5, 11
Fluorite	1, 2, 11
Muscovite	1, 2, 11
Tourmaline	11
Rutile	11
Pyrite	1, 11, 12
Chalcopyrite	1, 2, 3, 5, 8, 9, 11, 12
Chalcocite	1, 12
Covellite	6, 12
Molybdenite	1, 11
Sphalerite	10
Galena	11
Aikinite	1, 2, 4, 5, 11, 12
Benjaminite	1, 2, 3, 4, 6, 7, 8, 9
Berryite	2, 6, 7, 8
Matildite	2, 7
Lindstromite	2, 9
Bismuthinite	4
Hammarite	6, 7, 11
Krupkaite**	7, 8, 9, 12
Gustavite	7, 8, 9, 12
Unnamed Bi-Pb-Hg-Ag-Cu sulfosalt 1 (Phase X)	11
Unnamed Bi-Pb-Hg-Ag-Cu sulfosalt 2 (Phase Y)	11
Coloradoite	11, 12
Cerussite	10, 11, 12
Anglesite	10, 11, 12
Bismoclite-daubreeite	10, 11, 12
Bismutite	12
Chalcanthite	12
Corkite	12
Ferrimolybdite	12
Goethite	12
Jarosite	12
Koechlinite	12
Sulfur	12

** composition as given is that of hammarite rather than krupkaite. References - (1) Shannon (1924), (2) Nuffield (1953), (3) Karup-Møller (1972), (4) Nuffield (1975), (5) Harris & Chen (1975), (6) Harris & Chen (1976), (7) Karup-Møller (1977), (8) Makovicky & Mumme (1979), (9) Karup-Møller & Makovicky (1979), (10) S. A. Williams, pers. comm., 1981, (11) This study, (12) Dunning et al., (in press).

Sulfosalts and sulfides from the Outlaw prospect, northeast of Manhattan

Table 8 is a summary of minerals identified from this prospect. Despite the complexity and degree of difficulty in positively identifying the various sulfosalts that are present, only one mineral that was first identified as one species (pavonite) has been subsequently re-identified as another (benjaminite) (Karup-Møller 1972, 1977). Re-examination of various samples through the years has resulted in additional species being identified (*e.g.*, Nuffield 1953, 1975).

The aikinite–bismuthinite series. Four of the nine currently known members of the aikinite-bismuthinite series (*aikinite*, friedrichite, *hammarite, lindströmite*, krupkaite, gladite, unnamed member, pekoite, and *bismuthinite*) have been identified from the Manhattan–Round Mountain area. Details of the compositional and structural variations in the series have been provided only recently (Syneček & Hybler 1974, Žák *et al.* 1974, Mumme 1975, Harris & Chen 1976, Mumme & Watts 1976, Mumme *et al.* 1976, Chang & Hoda 1977, Horiuchi & Wuensch 1977, Chen *et al.* 1978, Makovicky & Makovicky 1978, Mozgova 1979, Prachař 1979, Žák 1980, Žák & Hybler 1981, Žák & Prachař 1981). Whereas a complete solid solution exists between aikinite and bismuthinite, there are distinct structural differences among different members of the series. Stoichiometric and nonstoichiometric compositions are composed of various cells of bismuthinite-type, krupkaite-type, and aikinite-type structural ribbons (Kostov & Minčeva-Stefanova 1982). Various members of the series, *e.g.*, pekoite and hammarite, may be seleniferous (*e.g.*, Mumme & Watts 1976, Kovalenker *et al.* 1984, Chekalova & Slyusarev 1974).

Aikinite. In this study, aikinite and possibly friedrichite(?) were identified from seven different samples from the Outlaw prospect. Electron-microprobe data on the aikinite and friedrichite(?) in all of these samples are given in Table 9. The compositions given in Table 9 and the average (of 7 samples) are plotted on Figure 8. Whereas some of the analytical points cluster around ideal friedrichite (Pb 30.5, Bi 43.1, Cu 9.4, S 17.0 wt.%), and other points are closer to ideal friedrichite than to ideal aikinite (Pb 36.0, Bi 36.3, Cu 11.0, S 16.7 wt.%), single-crystal precession-camera studies (of DRS-79-84a) confirmed that some material is nonstoichiometric aikinite with *a* 11.31(1), *b* 11.61(1), *c* 4.02(1) Å. Figure 9 is a photograph of a kinked (twinned) single crystal of aikinite (DRS-79-84a) elongated on *c* and striated parallel to [*c*]. Reddish brown internal reflections are present in oblique incident light. Our investigation showed only aikinite, friedrichite(?), and hammarite to be present as representative of the aikinite–bismuthinite series. Other investigators have reported lindströmite, krupkaite, and bismuthinite as well (Table 8). The composition of krupkaite (average of seven points) reported by Karup-Møller (1977) and Karup-Møller & Makovicky (1979) is just about identical to that reported by Harris & Chen (1976) as hammarite. Compositionally, the average of the seven points plots close to ideal hammarite and is quite removed from ideal krupkaite.

One specimen (FC-Benj) of material labelled "benjaminite, Outlaw Mine, Mariposa Canyon, Nye Co., Nev." was obtained from F. Cureton. This sample was collected in the 1920s from the Outlaw prospect. As viewed megascopically, the specimen consists of milky quartz containing muscovite, molybdenite, pyrite, and a bronze-tarnishing sulfosalt. Examination of the sulfosalt by electron microprobe showed the presence of a member of the aikinite–bismuthinite series having a composition nearly identical to that of ideal friedrichite (Table 9, Fig. 8). The mineral, however, may be nonstoichiometric aikinite, as was found in some of the other samples examined in this study (Table 9, Fig. 8). One composition (Table 9, Fig. 8) lies midway between friedrichite and hammarite, which is probably a nonstoichiometric hammarite. One area examined by microprobe contains a 20-μm-wide veinlet of a mercury-bearing Bi–Pb–Ag–Cu sulfosalt (phase X), which is most likely a new species. Material of similar composition was found in two additional samples (DRS-73-43b and DRS-73-43d); additional details are given later.

One sample (DRS-73-43a) of aikinite from the Outlaw prospect contains 100 ppm As, 150 ppm Sb, 200 ppm Se, 50 ppm Hg, 100 ppm Te, and 7 ppm Tl (emission-spectrographic determination of chalcophile elements by C. Heropoulos, USGS). Six-step semiquantitative emission-spectrographic analysis (NMC) of another split of this sample showed: Fe 0.15%, Ag 3000 ppm, Ba 15 ppm, Bi major, Cu major, Pb major, Cr 7 ppm, Ni 10 ppm, Mo 500 ppm, Sb 700 ppm, and 1.5% Si. No other elements were detected.

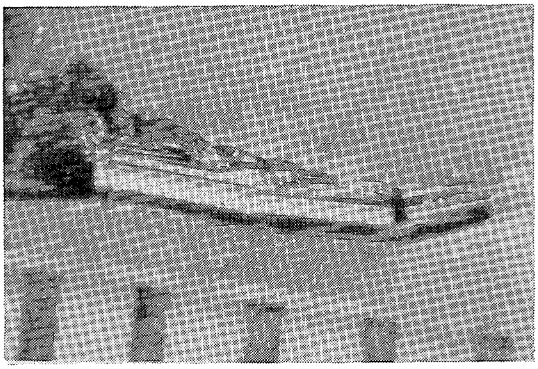

FIG. 9. Photograph of kinked, elongate, striated crystal of aikinite in quartz from the Outlaw prospect (DRS-79-84a), Mariposa Canyon, Toquima Range, Nevada. Scale divisions are 1 mm.

What is most likely aikinite, with a slight excess of bismuth, is present in DRS-80-38a (prospect 2 km southeast of Round Mountain; Table 9) associated with sphalerite, pyrite, and quartz. An emission-spectrographic analysis (NMC) of the aikinite(?) that contains minor sphalerite and pyrite shows 300 ppm Ag and 3000 ppm Sb. Among the chalcophile elements (analyst: C. Heropoulos), the sample contains 50 ppm As, <1 ppm Hg, 2 ppm Tl, 70 ppm Te, 700 ppm Se, 500 ppm Sb, and < 0.2 ppm Au. The associated sphalerite (containing about 4% aikinite) contains 0.5% Fe, 0.3% Mn, 1.5% Cd, 50 ppm In, and 7 ppm As.

TABLE 9. ELECTRON MICROPROBE DATA FOR AIKINITE, FRIEDRICHITE(?), AND HAMMARITE FROM THE OUTLAW PROSPECT, MARIPOSA CANYON, AND THE PROSPECT SOUTH OF ROUND MOUNTAIN, TOQUIMA RANGE, NEVADA

Element	DRS-73 -43a	DRS-73 -43c	DRS-73 -43d	DRS-73 -43e	DRS-73 -43f	DRS-79 -84a	FC-BENJ		Average of Outlaw samples	DRS-80 -38a
No. of points	(4)	(2)	(2)	(3)	(2)	(2)	(2)	(1)		(3)
Cu	9.4	9.4	8.5	9.7	8.9	9.1	9.5	8.7	9.2	10.2
Sb	0.1	0.1	0.1	0.1	0.0	0.1	0.1	0.1	0.1	0.4
S	16.7	17.8	16.8	17.1	17.4	17.4	16.9	17.0	17.1	17.3
Pb	31.8	31.7	29.7	32.2	29.2	31.5	29.8	28.8	30.6	33.5
Bi	42.3	39.2	44.2	38.7	42.5	40.8	44.0	47.1	42.4	38.45
Ag	0.0	0.0	0.1	0.0	0.0	0.1	0.1	0.1	0.0	0.0
Zn	---	---	---	---	---	---	---	---	---	0.1
Te	N.D.	N.D.	N.D.	N.D.	N.D.	N.D.	.0	.1	0.0	N.D.
Total	100.3	98.2	99.4	97.9	98.0	99.0	100.4	101.9	99.4	99.95

Note: Zn, Fe, and As sought but not detected above limit of determination in Outlaw prospect samples. N.D., not determined. Mo and Hg sought but not found in DRS-73-43a, and DRS-73-43d. DRS-73-43a-43f, DRS-79-84a, FC-BENJ - Outlaw prospect; DRS-80-38a prospect south of Round Mountain.

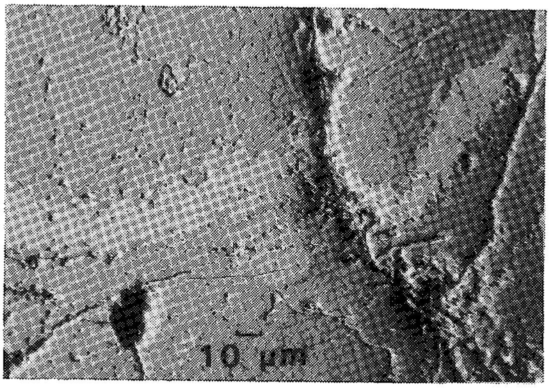

FIG. 10. BSE photograph of veinlet of unidentified Hg-bearing sulfosalt within aikinite. DRS-73-43d, Outlaw prospect, Mariposa Canyon, Toquima Range, Nevada. Dark grey aikinite host, light grey Hg-bearing Pb–Bi–Ag–Cu sulfosalt.

Results of electron-microprobe analyses of the aikinite(?) are given in Table 9. The average of the three data-sets, plotted on Figure 8, lies between theoretical aikinite and friedrichite, about 1/3 of the way from aikinite to friedrichite. No single-crystal X-ray studies were done on this material; the species designation is based on chemistry only.

Hammarite. An electron-microprobe analysis of one area in sample DRS-73-43d (Outlaw prospect) gave a composition very close to that of hammarite: Cu 7.05, Sb 0.22, S 16.74, Pb 26.22, Bi 49.97, Fe 0.10, Mo 0.09, Hg 0.23, total 100.43 (Fig. 8). Zinc, silver, and arsenic were sought but not detected. The results are in agreement with the findings of Harris & Chen (1976) and Karup-Møller (1977) on hammarite from the Outlaw prospect.

Phase X (probably a new Bi–Pb–Hg–Cu sulfosalt). Three of the eight polished sections examined from the Outlaw prospect (DRS-73-43b, DRS-73-43d, and FC-Benj) contain a mercury-bearing sulfosalt mineral, here called phase X. Phase X has been observed only as veinlets that cut nonstoichiometric aikinite (in two samples, FC-benj and DRS-73-43d). The reflectivity and color differences between phase X and aikinite are very small, but the carbon applied for microprobe analysis enhanced these differences. BSE photographs show the intergrowth of the mercury-bearing sulfosalt and aikinite very clearly (Fig. 10). The mercury-bearing sulfosalt has veined and replaced the aikinite. The presence of mercury in the sulfosalt was confirmed by wavelength spectrometer scans and subsequently by emission-spectrographic analysis (NMC). The presence of mercury was noted in the bulk sample of aikinite from the Outlaw prospect (DRS-73-43), but not in the aikinite(?) from the prospect 2 km southeast of Round Mountain (DRS-80-38a). Mercury also has been detected at low levels (20 to 50 ppm) by spectrographic determination of the chalcophile elements, in samples of tetrahedrite–tennantite (DRS-78-1, DRS-78-2, DRS 74-243), and in one sample of sphalerite (DRS-74-252a) from sulfide- and sulfosalt-mineralized hübnerite–quartz veins described by Shawe *et al.* (1984). This study also has indicated the presence of mercury in a sample of sphalerite from the prospect 2 km southeast of Round Mountain (20 ppm, DRS-80-38a) and in the composite sulfosalt from one of the prospects north of the White Caps mine (15 ppm, DRS-80-56).

Electron-microprobe data for the mercury-bearing sulfosalt in DRS-73-43b and DRS-73-43d for 11 elements are given in Table 10. If these compositions (and the average) are plotted on a triangular diagram Ag(+Cu)–Bi–Pb (Fig. 4) adding Hg to the Ag + Cu corner, they fall very near the N equals 7 line (N_{chem} = 7.16) and lie between eskimoite and heyrovskyite, but are closer to eskimoite. The metal-to-sulfur ratio for phases along this line is 0.889. Table 11 summarizes data on phases lying along this line.

A complete structural formula of phase X based on 27 sulfur atoms is: $(Hg_{2.23}Ag_{1.40}Cu_{1.05}Pb_{0.32})(Pb)_{8.0}(Bi_{10.71}Mo_{0.06}Pb_{0.05}Sb_{0.02})S_{27}$. Single-crystal studies of the material will be necessary to determine if it is a mercury-substituted heyrovskyite, a mercury-substituted eskimoite, a new member of the lillianite homologous series, or a new species.

Phase Y (probably a new Bi–Pb–Hg–Ag–Cu sulfosalt). Either a compositional variant of phase X (N = 7) or, more likely, a new species of similar composition but with N equal to 11 was found in DRS-73-43b. Two microprobe analyses of the mineral gave: Sb 0.02, 0.03; Te 0.04, 0.07; Cu 1.60, 1.61; Hg 10.13, 9.14; S 15.40, 15.42; Pb 35.04, 34.71; Bi 36.79, 36.95; Ag 2.59, 2.43; total 101.61, 100.37 wt.%. Iron, zinc, and arsenic were looked for but not detected. These compositions are plotted on Figure 4. This mineral forms the bulk of one area (about 200 × 200 μm) in the section, and contains lath-like intergrowths of phase X (Table 10), exsolved blebs and irregular masses of galena, and coloradoite. Phase Y has been found in only one section thus far, and may possibly be a mercury- and copper-substituted ourayite; single-crystal X-ray-diffraction studies will be necessary to completely characterize the mineral.

It seems clear that a mercury-rich and, to a lesser extent, a silver-bearing mineral assemblage postdates an earlier Bi–Pb–Cu–Mo–Fe mineral assemblage at the Outlaw prospect. Phase X occurs as veinlets in earlier formed minerals but as intergrown laths in the later generation of mercury-, silver-rich, and copper-poor minerals.

Coloradoite. Based on microprobe analyses, very minor amounts of coloradoite, HgTe, were identified in sample DRS-73-43b. The mineral occurs as irregular and randomly oriented blebs (grains) as much as 15 × 20 μm in size included within phase Y. Recently, this mineral also has been identified from the Outlaw prospect by Dunning *et al.* (1988). Insufficient amounts were available for X-ray-diffraction studies.

Benjaminite. Benjaminite, first described (Karup-Møller & Makovicky 1979, Makovicky & Mumme 1979) from the Outlaw prospect, was not found during this investigation (Table 8). The existence of a copper- and lead-unsubstituted benjaminite from Australia was described by Herbert & Mumme (1981).

Galena. Galena, not previously reported from the Outlaw prospect, was found in one sample (DRS-73-43b). Some of this galena, however, rather than having the coupled $Ag + Bi \rightleftharpoons 2Pb$ substitution, appears to illustrate a $Hg(Ag) + Bi \rightleftharpoons 2Pb$ coupled substitution. Two analyses of an elongate intergrowth of galena in phase Y within DRS-73-43b gave: Cu 0.1, 0.1; S 13.3, 13.6; Pb 83.9, 83.3; Bi, 0.9, 0.8; Ag 0.45, 0.40; Sb 0.1, 0.0; Hg 0.1, 0.0; total 98.85, 98.2 wt.%. No antimony, tellurium, or zinc was detected. The grain shows the normal $Ag + Bi \rightleftharpoons 2Pb$ coupled substitution. Two other microprobe analyses of galena from the same sample gave: Cu 0.17, 0.14; S 13.2, 13.9; Pb 76.3, 78.9; Bi 4.3, 4.9; Ag 0.7, 0.6; Hg 5.0, 1.3; totals 99.67, 99.74 wt.%. A structural formula based on one sulfur atom, using the average of the two analyses is: $(Pb_{0.88}Bi_{0.05}Hg_{0.04}Ag_{0.01})S$.

Alteration products of sulfides and sulfosalts. Identified products of alteration of galena from the Fairview mine material are covellite, anglesite, and cerussite. These same minerals are also present at the other galena-bearing localities examined.

A mineral(s) that shows low reflectivity, is medium-dark grey in reflected light and light to medium yellow in plane light, occurs as an alteration product that coats, fills fractures, and is included within galenobismutite and gustavite in DRS-80-56. Two microprobe analyses showed: Bi 86.0 and 86.5% and S 0.0 and 0.1%, respectively; totals 86.0 and 86.6 wt.%. No other elements above atomic number 9 (F) were detected. This mineral is most likely bismite, bismutite, or daubreeite–bismoclite.

An emission-spectrographic analysis (NMC) of a bismutite–anglesite mixture associated with aikinite, sphalerite, pyrite, and quartz (DRS-80-38a) gave: Fe 0.2%, Mg 0.01%, Ca 1.5%, Mn 5 ppm, Ag 700 ppm, Ba 200 ppm, Bi >10%, Cd 70 ppm, Cr 30 ppm, Cu 1000 ppm, Mo 7000 ppm, Ni 15 ppm, Pb >10%, Sb 3000 ppm, Sr 100 ppm, U 1000 ppm, V 500 ppm, Y 30 ppm, Zn 700 ppm, Si 3%, Al 0.3%, and Yb 3 ppm. All other elements were not detected at respective limits of determination (Table 5). The host(s) of the calcium, uranium, vanadium, and molybdenum have not been established.

TABLE 10. ELECTRON MICROPROBE ANALYSES OF MERCURY-BEARING SULFOSALT FROM THE OUTLAW PROSPECT, MARIPOSA CANYON, TOQUIMA RANGE, NEVADA

Element	DRS-73-43b		DRS-73-43d			Average of 1-3
	A	B	1	2	3	
Cu	1.3	1.3	1.5	0.9	1.3	1.2
Sb	0.3	0.0	0.1	0.1	0.1	0.1
S	15.9	16.0	16.0	15.6	15.8	15.8
Pb	29.8	29.3	30.6	32.3	31.8	31.6
Bi	40.3	40.6	42.1	39.7	40.5	40.8
Ag	3.4	3.6	2.7	3.1	2.5	2.8
Mo	n.d.	n.d.	0.0	0.2	0.1	0.1
Hg	8.3	8.4	9.0	7.7	7.7	8.1
Te	0.3	0.4	n.d.	n.d.	n.d.	----
Totals	99.3	99.3	102.0	99.6	99.9	100.5

Note: Fe, As, and Zn sought but not detected above limits of determination. n.d., not determined

TABLE 11. MINERALS HAVING N = 7 IN THE SYSTEM Pb – Bi(Sb) – Ag(Cu)(Hg)

Mineral	Formula	Metal/sulfur
eskimoite	$Ag_7Pb_{10}Bi_{15}S_{36}$	32/36 = 0.889
phase X	$(Hg,Ag,Cu,Pb)_5Pb_8(Bi,Pb,Sb,Mo)_{11}S_{27}$	24/27 = 0.889
heyrovskyite	$Pb_6Bi_2S_9$ to $Pb_{10}AgBi_5S_{18}$	8/9 or 16/18 = 0.889
aschamalmite	$Pb_6Bi_2S_9$	8/9 = 0.889
schirmerite	$Ag_3Pb_6Bi_7S_{18}$ (low Pb, high Ag; low end)	16/18 = 0.889

A white to creamy microcrystalline crust (alteration coating) on aikinite in DRS-79-84b from the Outlaw prospect also was examined. A six-step emission-spectrographic analysis (NMC) of a 3.3 mg bulk sample gave: Fe 0.05%, Mg 0.02%, Ca 0.1%, Mn 5 ppm, Ag 200 ppm, Ba 500 ppm, Bi >10%, Cu 500 ppm, La 200 ppm, Mo 30 ppm, Pb 2%, Sr 50 ppm, Al <150 ppm. All other elements were not detected (Table 5). Transmitted-light and X-ray-diffraction studies of this material indicate anglesite and probable bismoclite–daubreeite. Additional alteration products of sulfides and sulfosalts are listed in Table 8.

DISCUSSION AND CONCLUSIONS

In many natural deposits and in synthetic systems involving lead–bismuth sulfides and sulfosalts, a generalized paragenetic sequence has been observed in which lead-rich minerals form prior to bismuth rich ones (*e.g.*, Chang & Bever 1973, Czamanske & Hall 1975). Structurally, most bismuth sulfosalts are composed of axial-type structures (Kostov & Minčeva-Stefanova 1982). Furthermore, a trend exists from bismuth to antimony to arsenic sulfosalts with generally decreasing temperature. Antimonian sulfosalts are principally of pseudo-isometric types, and arsenian sulfosalts are principally planar types. This trend, axial → pseudo-isometric → planar, has a definite bearing on the conditions of crystallization of the respective sulfosalt minerals. The sulfosalt minerals tend to separate and crystallize after the sulfide minerals (Kostov & Minčeva-Stefanova 1982).

However, within the Pb–Bi–Ag–(Cu)–S system, some minerals, such as the crystallization sequence bismuthinite, galenobismutite, lillianite–gustavite, berryite(?), and galena$_{ss}$, which have been investigated in this study, commonly exhibit progressive lead-enrichment or silver-enrichment (or both) with decreasing temperature (Karup-Møller 1977). Ontoyev *et al.* (1982) found similar results in their study of members of the lillianite–gustavite series and related sulfosalts. Silver- and bismuth-rich sulfosalts formed earliest, then sulfosalts with a moderate amount of these elements, and finally at the end, galena with an insignificant content of silver and bismuth. As stated by Malakhov (1968) and Karup-Møller (1977), bismuth-bearing sulfides are generally considered to have crystallized in the high-temperature hydrothermal range, antimony-bearing sulfides in the medium hydrothermal range, whereas arsenic-bearing sulfides generally belong to the low-temperature hydrothermal (epithermal) ranges. Abundant data including phase equilibria (*e.g.*, Craig 1967), fluid inclusions (*e.g.*, Nedachi *et al.* 1973), stable isotopes, and other data indicate that most of the mineral parageneses belonging to the Pb–Bi–Ag–(Cu)–S system have crystallized at temperatures between 200 and 400°C. Galena + Pb–Bi–Ag(Cu) sulfosalt assemblages at Ivigtut, Greenland are interpreted to have crystallized between 300 and 550°C (Karup-Møller 1973, 1977, Karup-Møller & Pauly 1979). Galena and associated sulfosalts in the Darwin district, California were interpreted to have crystallized at more than 350°C (Czamanske & Hall 1975).

The annealing of samples with high bismuth contents (21 to 27 wt.% Bi) and that do not lie on the galena–matildite join (*i.e.*, being composed of matildite, clausthalite, and galena) at 500°C for 5 hours produces a galena-type pattern (Czamanske & Hall 1975). This is due to reincorporation of the other elements into the high-temperature galena structure.

Galenobismutite has been determined to be stable above about 390°C (Hoda & Chang 1975, Chang & Hoda 1977). Below this temperature, decomposition to bismuthinite and lillianite occurs: $3PbBi_2S_4 \rightarrow 2Bi_2S_3 + Pb_3Bi_2S_6$. Galenobismutite was found at only one locality (DRS-80-56) examined in the Round Mountain - Manhattan area. Only bismuthinite is directly associated (intergrown) with the galenobismutite. As mentioned in earlier pages, another part of the same polished section contains gustavite and bismuthinite. Deposition of the galenobismutite and bismuthinite as interlocking euhedral crystals indicates that the bismuth (+silver?) mineralization took place above 390°C, if the stability data of Chang & Hoda (1977) are used as a geothermometer.

Bismuth and antimony contents of 204 samples of galena from 84 deposits representing a depth range of crystallization from 300 to 5000 m were examined by Malakhov (1968). He concluded that the Sb:Bi ratio principally reflects the temperature of crystallization of the galena. Very low Sb:Bi values (<0.06) are characteristic of high-temperature galena (200–300°C and greater), whereas higher Sb:Bi values (>6.0 to 13) are typical of low-temperature galena (100–160°C).

Values of the Sb:Bi ratio in galena from the Round Mountain and Manhattan gold districts range from 0.00x to 5 (6-step semiquantitative emission-spectrographic analyses), <0.0001 to 8 (quantitative emission-spectrographic analyses), 0.03 to 7 (chalcophile-element emission-spectrographic analysis), and from 0.01 to 25 (electron-microprobe analysis). These values are in agreement with the range of temperatures and depths of formation estimated for these districts from geological and laboratory (fluid-inclusion data) studies: depth about 3 km, temperature 300–200°C, to depth less than 1 km and temperature less than 200°C (Nash 1972, Shawe *et al.* 1984). Significantly, the values for galena from the Round Mountain and Manhattan districts show wide variation and, moreover, two populations, one with values greater than 2 and the other with values less than 1. Samples of galena from one locality (Lead-Silver King prospect) have two distinct chemical compositions, based on major-, minor-, and trace-element contents, as well as two distinct habits (fillings in sheared quartz, and as irregular tabular crystals in quartz vugs). The two samples (DRS-79-18 and DRS-74-142b) have low silver and bismuth contents and elevated antimony contents relative to those of DRS-74-142a, which has high silver and bismuth and low antimony. Thus, two generations of galena appear to be present, a high-temperature form and a low-temperature form.

Khetchikov (1958) found two generations of galena in a polymetallic skarn deposit in the Soviet Far East: the first is high in bismuth and is early, whereas the second has no bismuth and is late. However, within the first generation of galena, great heterogeneity (as much as 2 wt.% Bi difference) was found from closely spaced samples within the same type of ore. This heterogeneity was attributed to inclusions of galenobismutite. The two generations of galena from the Kti-Tberda deposit, northern Caucasus, U.S.S.R. (Ontoyev *et al.* 1982), deposited in Paleozoic and Mesozoic time, respectively, are another example of two distinctly separate episodes of mineralization.

Galena is definitely not always the simple mineral that it commonly is assumed to be. Galena may under appropriate conditions contain substantial amounts of silver and bismuth (with lesser antimony) in solid-solution (as much as 25 mol.% $AgBiS_2$), without decomposition to matildite plus silver- and bismuth-free galena. The substitutional scheme

$2Pb^{2+} \rightleftharpoons Bi^{3+} + Ag^{+}$ has been accepted by many investigators to account for the presence of silver and bismuth in galena. However, as noted by Karup-Møller (1977), any surplus of silver over bismuth (in single-phase galena) would require, in order to maintain charge balance, the insertion of $2Ag^{+}$ for each Pb^{2+} removed. One of the two silver atoms would therefore have to be placed in interstitial positions in the galena structure. However, as also noted by Karup-Møller (1977), such positions are apparently not available, accounting for the apparent impossibility of finding more than a few tenths of a mol.% silver in excess of bismuth. An excess of bismuth is readily accounted for, because for every $3Pb^{2+}$ removed, $2Bi^{3+}$ enter into the galena structure, leaving one lead position empty. If a substantial excess of bismuth is present, and no other bismuth-bearing minerals are present, then a domain structure may exist. Such domain structures may be similar to those of the lillianite homologues (Karup-Møller 1977). Multiple generations of galena are restricted to base- and precious-metal deposits where sufficient amounts of silver and bismuth both are present in lead-rich environments. We believe that these galenas originate by either incomplete exsolution resulting from rapid cooling, or by multiple heating (mineralizing) events in varied geochemical environments.

The presence of coexisting galenas with or without associated Pb–Bi–Ag(Cu) sulfosalt assemblages supports the geological and geochronological evidence for multiple and chemically complex stages of mineralization in the Round Mountain and Manhattan districts. They also may be used as crudely approximate geothermometers.

The Round Mountain and Manhattan districts are areas in which several distinct and separate episodes of base- and precious-metal mineralization took place over approximately 65 Ma (80 to 15 Ma). Following emplacement of granite plutons, a variety of small, mostly uneconomic base- and precious-metal veins and tungsten-bearing tactite and vein deposits formed at 80–75 Ma in the granite and in nearby Paleozoic carbonate and clastic rocks (Shawe *et al.* 1984, 1986, Shawe 1985, 1986). These deposits are characterized by small amounts of simple sulfides: pyrite, sphalerite, chalcopyrite, and galena. The quartz–hübnerite veins in granite were subsequently remineralized with copper, lead, zinc, arsenic, and antimony in the vicinity of a 35 Ma granodiorite stock and associated rhyolite dyke-swarm. Deposition of Pb–Bi–Ag(Cu) sulfides and sulfosalts, as well as tetrahedrite–tennantite, and the replacement of galena by covellite, are thought to have been associated with this event. Possibly two separate events, an early bismuth-rich event (a late phase of the hübnerite episode, at 80 Ma?), and a late tetrahedrite–tennantite event (at 35 Ma), took place. The main gold–silver mineralization at Round Mountain occurred at 25 Ma within a rhyolitic ash-flow tuff. This mineralizing event, by modification of an older (Cretaceous?) vein, may have been responsible for production of the two coexisting compositions of PbS_{ss} at the Fairview mine. The two distinctly different compositions of galena found at the Lead-Silver King prospect are probably products of Tertiary events younger than the 27 Ma tuff of Mount Jefferson that forms one wall of the Lead-Silver King vein system. An economically significant gold–silver mineralizing event at Manhattan took place at 16 Ma within Paleozoic sedimentary rocks along the south margin of the Manhattan caldera. A separate but undated (probably early) Tertiary mineralizing event introduced mercury, antimony, and arsenic minerals into the eastern part of the Manhattan belt (a northeast-trending zone centered on the White Caps mine: Shawe 1986). Other centers of mercury, antimony, and arsenic mineralization peripheral to the Manhattan caldera may have formed concurrently. Formation of the mercury-bearing Bi–Pb–Ag–Cu sulfosalts (phases X and Y), coloradoite, and the mercurian galena in a Cretaceous quartz vein at the Outlaw prospect is thought to have occurred during this episode of mineralization.

Thus, we infer a general sequence of deposition of sulfides and sulfosalts in the Round Mountain – Manhattan area, although timing of the sequence is imperfectly known, and similar stages in different localities may not be strictly correlated in time. Isotopic ages have not been determined on any of the lead minerals. Interpretations of lead-isotope analytical data would of course depend on assumptions that may or may not be valid for the complex mineralized environments in the two gold districts. An early high-temperature event related to the Cretaceous granite plutons involved deposition of simple sulfides in tactites and quartz veins. At a later time, a high-temperature bismuth-, silver-rich hydrothermal activity locally modified these deposits. Probably at about 35 Ma a lower temperature copper–lead–zinc–arsenic–antimony mineralization (characterized by covellite replacement of galena and tetrahedrite–tennantite deposition) related to the granodiorite stock and associated rhyolite dyke-swarm modified some of the Cretaceous veins. Still later, at about 25 Ma and at 16 Ma, low-temperature gold mineralization occurred at Round Mountain and at Manhattan, further modifying older deposits in those areas. A Tertiary mercury–arsenic–antimony low-temperature event also modified older deposits in the vicinity of the White Caps mine, the Outlaw prospect, and at other centers peripheral to the Manhattan caldera.

Additional new mineral species in the Pb–Bi–Ag(Cu) ± Hg system continue to be reported. Many additional studies remain to be done on this system to further elucidate T, P, and fS_2 conditions of mineral deposition in complex natural systems.

ACKNOWLEDGEMENTS

The authors thank C. Heropoulos (U.S. Geological Survey, Menlo Park, Calif.) for emission-spectrographic analyses for the chalcophile elements on selected minerals and mineral mixtures. We are grateful to James Craig (V.P.I., Blacksburg, Va.) for sealing some galena and sulfosalt samples in quartz tubes under vacuum and annealing them for us. One sample of 'benjaminite' from the Outlaw prospect was provided by Forrest Cureton. The staff of the U.S. Geological Survey library was most helpful in obtaining many of the Russian language publications used in this work. We gratefully acknowledge the careful and perceptive reviews of R. C. Erd, P. J. Modreski, and B. F. Leonard, all of the U.S. Geological Survey. We also acknowledge the constructive reviews of two anonymous referees and the editor of the Canadian Mineralogist, R. F. Martin.

REFERENCES

BORODAYEV, YU. S. & MOZGOVA, N.N. (1971): New group of the sulfobismuthides of Ag, Pb and Cu. *Soc. Mining Geol. Japan, Spec. Issue.* (Proc. of IMA-IAGOD meetings '70, joint symp.) **2**, 34-41.

CHANG, L. L. Y. & BEVER, J. E. (1973) Lead sulphosalt minerals: crystal structures, stability relations, and paragenesis. *Minerals Sci. Eng.* **5**, 181-191.

______ & HODA, S. N. (1977): Phase relations in the system $PbS-Cu_2S-Bi_2S_3$ and the stability of galenobismutite. *Amer. Mineral.* **62**, 346-350.

CHEKALOVA, K. A. & SLYUSAREV, A. P. (1974): Find of seleniferous hammarite in the Orlovskoye deposit, Rudnyy Altai. *Dokl. Acad. Sci. USSR, Earth Sci. Sect.* **216**, 144-146.

CHEN, T. T., KIRCHNER, E. & PAAR, W. (1978): Friedrichite, $Cu_5Pb_5Bi_7S_{18}$, a new member of the aikinite-bismuthinite series. *Can. Mineral.* **16**, 127-130.

CRAIG, J. R. (1967): Phase relations and mineral assemblages in the Ag-Bi-Pb-S system. *Mineralium Deposita* **1**, 278-306.

CZAMANSKE, G. K. & HALL, W. E. (1975): The Ag-Bi-Pb-Sb-S-Se-Te mineralogy of the Darwin lead-silver-zinc deposit, southern California. *Econ. Geol.* **70**, 1092-1110.

DUNNING, G. E., COOPER J. F., JR. & MOSS, G. E. (1988): Rediscovery of the Outlaw mine, Nye County, Nevada. *Miner. Rec.* (in press).

FERGUSON, H. G. (1921): The Round Mountain district, Nevada. *U.S. Geol. Surv. Bull.* **725-I**, 383-406.

FINASHIN, V. K., LITAVRINA, R. F., ROMANENKO, I. M. & CHUBAROV, V. M. (1981): On lillianite-gustavite and the lillianite-gustavite mineral series in tin ores of the Kavalerovsk region. *Zap. Vses. Mineral. Obshch.* **110**, 304-310. (In Russ.).

FOORD, E. E., SHAWE, D. R. & CONKLIN, N. M. (1985): Multiple coexisting phases of galena and associated sulfosalts from the southern Toquima Range, Nevada and the Idarado mine, Ouray, Colorado. *Geol. Soc. Amer. Program Abstr.* **17**, 219.

HARRIS, D. C. & CHEN, T. T. (1975): Benjaminite, reinstated as a valid species. *Can. Mineral.* **13**, 402-407.

______ & ______ (1976): Crystal chemistry and re-examination of nomenclature of sulfosalts in the aikinite-bismuthinite series. *Can. Mineral.* **14**, 194-205.

______ & OWENS, D. R. (1973): Berryite, a Canadian occurrence. *Can. Mineral.* **11**, 1016-1018.

HERBERT, H. K. & MUMME, W. G. (1981): Unsubstituted benjaminite from the AW Mine, NSW: a discussion of metal substitutions and stability. *Neues Jahrb. Mineral. Monatsh.*, 69-80.

HODA, S. N. & CHANG, L. L. Y. (1975): Phase relations in the systems $PbS-Ag_2S-Sb_2S_3$ and $PbS-Ag_2S-Bi_2S_3$. *Amer. Mineral.* **60**, 621-633.

HORIUCHI, H. & WUENSCH, B. J. (1977): Lindströmite, $Cu_3Pb_3Bi_7S_{15}$: its space group and ordering scheme for metal atoms in the crystal structure. *Can. Mineral.* **15**, 527-535.

KARUP-MØLLER, S. (1966): Berryite from Greenland. *Can. Mineral.* **8**, 414-423.

______ (1972): New data on pavonite, gustavite, and some related sulfosalt minerals. *Neues Jahrb. Mineral. Abh.* **117**, 19-38.

______ (1973): A gustavite-cosalite-galena-bearing mineral suite from the cryolite deposit at Ivigtut, South Greenland. *Medd. Grønland* **195(5)**.

______ (1977): Mineralogy of some Ag-(Cu)-Pb-Bi sulphide associations. *Bull. Geol. Soc. Denmark* **26**, 41-68.

______ & MAKOVICKY, E. (1979): On pavonite, cupropavonite, benjaminite and "oversubstituted" gustavite. *Bull. Minéral.* **102**, 351-367.

______ & ______ (1981): Ag- and Bi-rich heyrovskyite from the Bi-W-Mo mineralization at Castlegar, British Columbia. *Can. Mineral.* **19**, 349-353.

______ & Pauly, H. (1979): Galena and associated ore minerals from the cryolite deposit at Ivigtut, South Greenland. *Medd. Grønland, Geosci.*, 25 pp.

Khetchikov, L. N. (1958): On the question about the content of bismuth in galena. Soobshcheniya Dal'nevostoch. Filiala im. V. L. Komarova. *AN CCCP*, No. **9**, 133-136. Vladivostok. (In Russ.).

Kostov, I. & Minčeva-Stefanova, J. (1982): *Sulphide Minerals - Crystal Chemistry, Parageneses and Systematics*. E. Schweizerbart'sche Verlagsbuchhandlung, Stuttgart, W. Germany.

Kovalenker, V. A., Malov, V. S., Yevstigneeva, T. L. & Vyal'sov, L. N. (1984): Junoite and pekoite — first find in the USSR. *Zap. Vses. Mineral. Obshch.*113, 35-43.

Makovicky, E. & Karup-Møller, S. (1977a): Chemistry and crystallography of the lillianite homologous series. I. General properties and definitions. *Neues Jarhb. Mineral. Abh.* **130**, 264-287.

______ & ______ (1977b): Chemistry and crystallography of the lillianite homologous series. II. Definition of new minerals: eskimoite, vikingite, ourayite and treasurite. Redefinition of schirmerite and new data on the lillianite-gustavite solid solution series. *Neues Jahrb. Mineral. Abh.* **131**, 56-82.

______ & ______ (1984): Ourayite from Ivigtut, Greenland. *Can. Mineral.* **22**, 565-575.

______ & Makovicky, M. (1978): Representation of compositions in the bismuthinite–aikinite series. *Can. Mineral.* **16**, 405-409.

______ & Mumme, W. G. (1979): The crystal structure of benjaminite $Cu_{0.50}Pb_{0.40}Ag_{2.30}Bi_{6.80}S_{12}$. *Can. Mineral.* **17**, 607-618.

Malakhov, A. A. (1968): Bismuth and antimony in galenas as indicators of some conditions of ore formation. *Geochem. Int.* **7**, 1055-1068.

Mozgova, N. N. (1979): Nonstoichiometric and homologous series of sulfosalts. *Mineral. Zh.* **1**, 93-98. (In Russ.).

Mumme, W. G. (1975): The crystal structure of krupkaite, $CuPbBi_3S_6$, from the Juno mine at Tennant Creek, Northern Territory, Australia. *Amer. Mineral.* **60**, 300-308.

______ & Watts, J. A. (1976): Pekoite, $CuPbBi_{11}S_{18}$, a new member of the bismuthinite–aikinite mineral series: its crystal structure and relationship with naturally- and synthetically-formed members. *Can. Mineral.* **14**, 322-333.

______, Welin, E. & Wuensch, B. J. (1976): Crystal chemistry and proposed nomenclature for sulfosalts intermediate in the system bismuthinite–aikinite (Bi_2S_3–$CuPbBiS_3$). *Amer. Mineral.* **61**, 15-20.

Nash, J. T. (1972): Fluid-inclusion studies of some gold deposits in Nevada. *In* Geological Survey Research, 1972. *U.S. Geol. Surv. Prof. Paper* **800-C**, C15-C19.

Nedachi, M., Takeuchi, T., Yamaoka, K. & Taniguchi, M. (1973): Bi–Ag–Pb–S minerals from Agenosawa mine, Akita Prefecture, northeastern Japan. *Tohoku Univ., Sci. Rep., Third Series,* **12**, no. 1, 69-80.

Nuffield, E.W. (1953): Benjaminite. *Amer. Mineral.* **38**, 550-552.

______ (1954): Studies of mineral sulpho-salts. XVIII. Pavonite, a new mineral. *Amer. Mineral.* **39**, 409-415.

______ (1975): Benjaminite - a re-examination of the type material. *Can. Mineral.* **13**, 394-401.

______ & Harris, D. C. (1966): Studies of mineral sulpho-salts. XX. Berryite, a new species. *Can. Mineral.* **8**, 407-413.

Ontoyev, D. O., Druzhinin, A. V., Tsepin, A. I., Vyal'sov, L. N. & Basova, G. V. (1982): Minerals of the gustavite–lillianite series from the Kti-Teberda deposit (northern Caucasus). *Int. Geol. Rev.* **24**, 659-670.

Prachař, I. (1979): Aikinit z Krupky, CSSR. *Acta* Univ. Carolinae-Geol. No. **3-4**, 183-186. (In Czech.).

Shannon, E. V. (1924): Benjaminite, a new sulphosalt mineral of the klaprothite group. *Proc. U.S. Nat. Museum* **65**, art. 24.

Shawe, D. R. (1981a): Geologic map of the Round Mountain quadrangle, Nye County, Nevada. *U.S. Geol. Surv. Open-File Rep.* **81-515**, scale 1:24,000.

______ (1981b): Geologic map of the Manhattan quadrangle, Nye County, Nevada. *U.S. Geol. Surv. Open-File Rep.* **81-516**, scale 1:24,000.

______ (1985): Multiple episodes of mineralization in the southern Toquima Range, Nye County, Nevada. *In* USGS Research on Mineral Resources-1985, Program and Abstracts (K. Krafft, ed.). *U.S. Geol. Surv. Circ.* **949**, 48-49.

______ (1986): Complex history of precious metal deposits, southern Toquima Range, Nevada. *U.S. Geol. Surv. Open-File Rep.* **86-0459**.

______, Foord, E. E. & Conklin, N. M. (1984): Huebnerite veins near Round Mountain, Nye County, Nevada. *U.S. Geol. Surv. Prof. Pap.* **1287**.

______, Marvin, R. F., Andriessen, P. A. M., Mehnert, H. H. & Merritt, V. M. (1986): Ages of igneous and hydrothermal events in the Round Mountain and Manhattan gold districts, Nye County, Nevada. *Econ. Geol.* **81**, 388-407.

SYNEČEK, V. & HYBLER, J. (1974): The crystal structures of krupkaite, $CuPbBi_3S_6$, and of gladite, $CuPbBi_5S_9$, and the classification of superstructures in the bismuthinite–aikinite group. *Neues Jahrb. Mineral. Monatsh.*, 541-560.

ŽÁK, L. (1980): Isomorphism and polymorphism in the bismuthinite–aikinite group. *Neues Jahrb. Mineral. Monatsh.*, 440-448.

______ & HYBLER, J. (1981): Krupkaite (x = 1.3) from Dobsina, CSSR. *Neues Jahrb. Mineral. Monatsh.*, 206-214.

______ & PRACHAŘ, I. (1981): Estimation of chemical compositions of the bismuthinite derivatives from the lattice parameters. *Neues Jahrb. Mineral. Monatsh.*, 495-504.

______, SYNEČEK, V. & HYBLER, J. (1974): Krupkaite, $CuPbBi_3S_6$, a new mineral of the bismuthinite–aikinite group. *Neues Jahrb. Mineral. Monatsh.*, 533-541.

Received December 15, 1986; revised manuscript accepted June 29, 1987.